



Exploring the *in vitro* Antifungal Effect of Selenite (SeIV) and Nano-Selenium (SeNPs) Produced by ABT Culture on Five Fungi Species



CrossMark

Mohsen A. Zommara¹, Sherouq Sakar², El-Sayed B. Belal², Metwaly Salem³ and Nabil Algamal⁴

¹Dairy Science Department, Faculty of Agriculture, Kafrelsheikh University, Kafr El-Sheikh 33516, Egypt

²Agricultural Botany Department, Agricultural Microbiology, Faculty of Agriculture, Kafrelsheikh University, Kafr El-Sheikh 33516, Egypt

³Department of Agricultural Botany, Faculty of Agriculture, Kafrelsheikh University, Kafr El-Sheikh 33516, Egypt

⁴Dairy Research Department, Animal Production Research Institute, Agriculture Research Center, Ministry of Agriculture, Egypt

SELENIUM nanoparticles (SeNPs) exhibit excellent antifungal abilities and are seen as a good substitute for controlling different kinds of fungi. The aim of the present study is to explore the antifungal effect of SeNPs produced by green syntheses using sodium selenite (Na_2SeO_3) (SeIV) in MRS medium using the eco-friendly lactic acid bacteria (LAB) mixed ABT culture of *L. acidophilus*, *B. bifidum* and *S. thermophilus*, incubated at 37°C for 48 hr. The Potato Dextrose Agar (PDA) media was fortified with different concentrations (50, 100, 150, 200 ppm) of either Se(IV) or SeNPs and inoculated with 5 different species of fungi strains isolated from Ras cheese surface. The isolated fungi were *Aspergillus niger* (*Asp. niger*), *Penicillium citrinum* (*P. citrinum*), *Penicillium roqueforti* (*P. roqueforti*), *Rhizopus arrhizus* (*R. arrhizus*) and *Trichoderma spp.* The obtained results showed that the conversion of Se(IV) to SeNPs was complete at 200 ppm when incubated in the previously mentioned medium. The Se(IV) concentration had little impact on SeNPs diameter size. The smallest SeNPs particle diameter ranged from (45-65 nm) however, the largest one was (244-275 nm). Both of Se(IV) and SeNPs had antifungal effect compared to control. However, SeNPs was found to have more antifungal activity against the isolated fungi compared to Se(IV). This effect was evident at the lowest used concentration (50 ppm). SEM, TBARS assays, and MALDI-TOF was used to explore the mechanism(s) of the effect of the two types of selenium on the isolated fungi. At 200 ppm, Se(IV) causes significant lipid peroxidation in *P. roqueforti* with a TBARS value of 0.836 Abs. This is higher than that of SeNPs, which shows 0.582 Abs. In contrast, *Asp. niger* experiences the highest oxidative stress with SeNPs at 1.055 Abs, compared to Se(IV), which is at 0.512 abs. *P. citrinum* shows similar TBARS values for Se(IV) at 0.496 abs and SeNPs at 0.488 abs. *R. arrhizus* also displays similar results, with Se(IV) at 0.465 abs and SeNPs at 0.498 abs. *Trichoderma spp.* shows comparable resilience to both treatments, with Se(IV) at 0.467 abs and SeNPs at 0.483 abs. This highlights the different responses of strains to the biochemical effects of Se(IV) and the physical-oxidative effects of SeNPs. In conclusion, Se(IV) and SeNPs are promising antifungal agents with broad applications in agriculture and healthcare. Their multifaceted modes of action, especially through oxidative stress and membrane disruption, make them effective against a variety of fungi. SeNPs, in particular, offer a safer and more targeted alternative to conventional fungicides.

Keywords: *Asp. niger*, *P. roqueforti*, *P. citrinum*, *R. arrhizus*, *Trichoderma spp.*, Se(IV), SeNPs.

1. Introduction

Fungi are an extremely versatile class of organisms which can attack different hosts, causing many serious diseases (Seyedmousavi *et al.*, 2018). The importance of fungal infections in humans and animals has increased over the last two decades (Dworecka-Kaszak *et al.*, 2020). These diseases caused by fungi can be difficult to treat due to developing resistance to standard antifungal drugs (Fisher *et al.*, 2012, Yapar, 2014). The antifungal effect of selenium nanoparticles (SeNPs) has been extensively studied, showing promising results against various fungal species. Numerous further studies have focused on selenium nanoparticles' antifungal properties (El-Saadony *et al.*, 2021, Nile *et al.*, 2023, Serov *et al.*, 2023).

Microorganisms (bacteria, fungi, and viruses) are becoming resistant to contemporary antibiotics, antifungal medications, and antiviral medications. The goal of finding novel molecular structures to address the issue of therapy in bacterial, fungal, and viral pathogenesis is currently facing the scientific community. Nanoparticles of selenium

*Corresponding author e-mail: mzommara@agr.kfs.edu.eg

Received: 10/06/2025; Accepted: 15/07/2025

DOI: 10.21608/EJSS.2025.392979.2203

©2025 National Information and Documentation Center (NIDOC)

have antibacterial properties. There are quite a few uses for these nanoparticles in the biomedical sector. The antibacterial, antifungal, anticancer, antiviral, and antiparasitic qualities of SeNPs have been reviewed in a number of recent publications (Martínez-Esquivias *et al.*, 2021, Kopel *et al.*, 2022, Serov *et al.*, 2023). New, safe, non-toxic, and environmentally acceptable ways to produce SeNPs are provided via physicochemical processes, biological processes, and the synthesis of nanostructures using bacterial (Prokisch and Zommara, 2011) and fungal strains (Gharieb *et al.*, 2025) as well as a number of plant extracts. (Karthik *et al.*, 2024).

It should be mentioned that the primary focus of these works is thorough explanation of the antifungal processes of SeNPs when switching between different kinds of microorganisms. Because they harm crops, horticulture crops, and dairy products, particularly fermented ones like fermented milk and different kinds of soft, semi-hard, and hard cheeses, fungi pose a significant threat to agricultural products in general and dairy products in particular. Our study was focused in 5 different isolates belonging to the fungal genera *Trichoderma* (green mold), *Penicillium*, *Aspergillus* and *Rhizopus* commonly grow on crops, cheese and other foods. *Aspergillus* and *Penicillium* dominate food contamination, posing mycotoxin risks, while *Rhizopus* causes spoilage in fruits and bread. *Trichoderma* has lower incidence but is relevant in biocontrol. Effective management balances risk mitigation with beneficial applications (Pitt and Hocking, 2009, Hymery *et al.*, 2014, Kure and Skaar, 2019, Zhang *et al.*, 2020).

Asp. niger is a ubiquitous filamentous fungus belonging to the genus *Aspergillus*, widely recognized for its ecological, industrial, and medical significance (Sabino *et al.*, 2019, Ráduly *et al.*, 2020, Jangid *et al.*, 2024). Commonly found in soil, decaying plant material, and indoor environments (Mousavi *et al.*, 2016). This black mold thrives in warm, humid conditions and is known for its rapid growth and resilience. Characterized by its dark brown to black conidia (spores) and yellowish hyphae, *Asp. niger* plays a dual role in nature and human applications. Ecologically, it acts as a saprophyte, breaking down organic matter and contributing to nutrient cycling. Industrially, *Asp. niger* is a powerhouse, extensively used in biotechnology for the production of enzymes (e.g., amylases, proteases) and organic acids, most notably citric acid, which is critical in food, beverage, and pharmaceutical industries (Cairns *et al.*, 2018). Its ability to secrete large quantities of metabolites under controlled fermentation conditions has made it a model organism in industrial microbiology. However, *Asp. niger* also has a clinical dimension, as it can act as an opportunistic pathogen, causing aspergillosis in immunocompromised individuals, particularly through inhalation of its spores (Patterson *et al.*, 2016). Additionally, under specific conditions, certain strains may produce mycotoxins, such as ochratoxin A, posing potential risks to food safety (Cairns *et al.*, 2018, Moglad *et al.*, 2023, Schuster *et al.*, 2024).

There are more than 400 species of ascomycetous fungi in the genus *Penicillium*. *Penicillium* species are important for both natural ecosystems and commercial uses, like the synthesis of antibiotics like penicillin (Fleming, 1929). *P. roqueforti* is the most common fungus employed in the manufacturing of blue cheeses like Stilton, Gorgonzola, and Roquefort (Gobbetti *et al.*, 2015). Although, this fungus causes spoilage of other types of cheese and produce mycotoxins (ochratoxin A and patulin) which are considered as a health hazard (Perrone and Susca, 2017). One of the most important *Penicillium* species is *P. citrinum*. It is commonly found in soil, decaying vegetation, stored grains, and indoor environments. While it is a relatively fast-growing mold, it is particularly important because of its mycotoxin production and biotechnological potential (Silva *et al.*, 2021, Kamle *et al.*, 2022).

R. arrhizus, a filamentous fungus in the Mucorales order, is a cosmopolitan species prevalent in soil, decaying organic matter, and fermented foods. Known for its rapid growth and distinctive morphology. *R. arrhizus* contributes to nutrient recycling as a saprophyte, efficiently degrading complex organic substrates like starch and cellulose. *R. arrhizus* is significant for producing enzymes (e.g., amylases, lipases) and organic acids, notably fumaric acid, used in food and pharmaceutical applications (Bose and Pandey 2016). Its fermentation capabilities also make it valuable in traditional food production (Zhao and Chen 2019). However, its metabolic versatility is tempered by safety concerns, as certain strains can produce mycotoxins like rhizonins, posing risks to food safety. Also, *R. arrhizus* is a primary causative agent of mucormycosis, a rare but severe opportunistic infection affecting immunocompromised individuals, with high mortality rates due to its aggressive tissue invasion. Its spores, easily aerosolized, are a common infection vector in hospital settings. (Ghosh & Ray, 2011, Borman *et al.* 2012).

Trichoderma is a filamentous fungus belonging to the Hypocreaceae family, it is found in a variety of soil types worldwide. It includes opportunistic ascomycete species that are important to agriculture because of their capacity to manage soil-borne illnesses as well as certain plant diseases of the leaves and panicles (Woo *et al.*, 2023). On the other hand, *Trichoderma* species, especially *Trichoderma harzianum*, are the culprits behind green mold illness in mushrooms. This disease can seriously harm mushroom crops and is known to regularly contaminate mushroom substrates (Colavolpe *et al.*, 2015). *Trichoderma* is a minor but notable issue on cheese surfaces, primarily causing spoilage through discoloration and off-flavors. Its incidence is driven by environmental contamination in high-

humidity ripening conditions, with management focusing on sanitation, environmental control, and robust starter cultures. While not a mycotoxin concern, its presence affects cheese quality and marketability, particularly in artisanal production (Pitt and Hocking, 2009, Vázquez *et al.*, 2021).

SeNPs and Se(IV) show strong antifungal activity through different mechanisms than traditional antifungals like polyenes and azoles. SeNPs cause various types of damage by producing reactive oxygen species (ROS). These ROS harm fungal membranes, proteins, and DNA, and interfere with mitochondrial ATP production (Husen & Siddiqi, 2014). SeNPs also stop biofilm formation by lowering hyphal adhesion and reducing EPS production (Vahdati & Moghadam, 2020). They inhibit cytochrome P450 and glutathione reductase, which weakens fungal defenses (Kieliszek, 2019). SeIV mainly works at a biochemical level by inactivating thiol groups in enzymes, such as thioredoxin reductase. This disrupts the redox balance (Zhang *et al.*, 2020) and causes oxidative DNA breaks that block replication (Hosnedlova *et al.*, 2018). In comparison to polyenes and azoles, SeNPs have clear benefits, such as lower toxicity, biodegradability, and multifunctionality, including antifungal, antioxidant, and plant-growth-promoting effects. However, how well they work relies on accurate dosing and stability, since aggregation can decrease their effectiveness. Traditional agents may act faster and target better, but they do not offer the wider benefits and sustainability found with SeNPs. Ongoing improvements in SeNP production and delivery will strengthen their position as a next-generation antifungal option. SeNPs are better at causing physical and oxidative damage, while SeIV increases biochemical damage.

SeNPs and Se(IV) compounds, like selenite, are becoming useful in food preservation, healthcare, and agriculture because of their antifungal, antimicrobial, and antioxidant traits. SeNPs, especially those made using eco-friendly methods, have lower toxicity and better bioavailability compared to the more reactive Se(IV). This makes them a promising choice for sustainable uses. In food preservation, SeNPs can stop foodborne pathogens and biofilms, such as *Staphylococcus aureus* and *Candida albicans*, at concentrations of 12.5–100 µg/mL (Vahdati & Tohidi, 2023). They disrupt microbial cell membranes and prevent biofilm formation, making them perfect for antibacterial coatings in food packaging, which helps extend shelf life. SeNPs also reduce oxidative damage from mycotoxins like patulin, ensuring food safety. Their antioxidant qualities, shown by 79.2% DPPH radical scavenging at 100 µM, allow them to be used as additives in functional foods. While Se(IV) is antimicrobial, its higher toxicity makes it less suitable for food systems. In healthcare, SeNPs show potential as antimicrobial and anticancer agents (Zhang *et al.*, 2021). They can target bacterial and fungal biofilms formed by *Escherichia coli* or *Aspergillus* species, offering hope for treating infections that resist regular drugs. SeNPs' antioxidant effects lower oxidative stress, which supports their use in wound healing and tissue engineering. Furthermore, their low toxicity and ability to influence immune responses make them good candidates for drug delivery systems and cancer therapies, where they can cause death in cancer cells. Se(IV) also has antimicrobial abilities but is limited by toxicity concerns, necessitating careful dosing (Barkalina *et al.*, 2014). In agriculture, SeNPs fight phytopathogenic fungi like *Fusarium oxysporum*, preventing mycelial growth at 50–100 µg/mL and boosting plant defense by upregulating genes like LOX and PR1a. When applied to leaves, SeNPs reduced *Fusarium* rot in cucumbers by 96% and increased yields by 120%. They also encourage plant growth at low doses (<50 µM) and help with biofortification. Se(IV) can work against fungi at lower concentrations (1 ppm), but it poses a risk of phytotoxicity, making SeNPs a better option for sustainable crop protection (Wadhwani, *et al.*, 2016, Hamouda *et al.*, 2024).

Despite the advancements of using Se(IV) or SeNPs as promise antifungal, we still need to explore how SeNPs and SeIV compare in effectiveness and how they act differently against various fungal species. Most previous research has focused on single forms of selenium or individual fungal strains. This leaves a gap in understanding how these agents affect multiple fungi under the same conditions. This study aims to fill that gap by using scanning electron microscopy (SEM) and thiobarbituric acid reactive substances (TBARS) assays to assess SeNPs and SeIV at 200 ppm against five fungal strains belonging to the fungal genera *Trichoderma*, *Penicillium*, *Aspergillus* and *Rhizopus* commonly found on the surface of Ras cheese- a traditional Egyptian hard cheese- By revealing their antifungal mechanisms, this research helps advance the creation of targeted, eco-friendly antifungal methods for food safety, healthcare, and sustainable agriculture.

2. Materials and Methods

2.1. Bacterial growth measurement

The bacterial growth in the MRS cultured media was monitored at 2 hr. intervals for 12 hr., and then after 24, 48 and 72 hr. of incubation. The bacterial growth was estimated by measuring the absorbance at 650 nm -typically used as a proxy for bacterial growth- as it correlates with cell density (Ayad *et al.* 2004) and determination the pH value (3020 Jenway, England) of the cultured media.

2.2. Preparation of selenium nanoparticles (SeNPs)

The biosynthesis method was carried out as previously described by **Prokisch and Zommara (2011)**. The yoghurt ABT culture (*L. acidophilus*, *B. bifidum* and *S. thermophilus*) culture (CHR - Hansen's lab, Copenhagen, Denmark) was cultivated in de Man, Rogosa, Sharpe (MRS) media (Oxoid MRS Broth medium, Thermo Fisher Scientific Inc. Waltham, MA, USA) amended with 50, 100, 150 or 200 ppm of filter sterilized Se(IV) and incubated at 40°C for 72 hr. The medium color was turned to dark red which indicate the production of SeNPs.

2.3. SeNPs size determination

TEM (JEM-2100, JEOL Co., 3-1-2 Musashino, Akishima, Tokyo 196-8558, Japan) photographs of the cultured media after 72 h. of incubation and size determination of SeNPs were measured according to **Nagy *et al.*, (2016)**.

2.4. Isolation, purification and identification of the fungi strains

A sample of the fungal growth from the surface of Ras cheese was scraped off and diluted in a series (10^{-2} - 10^{-4}) on selective medium (PDA). The hyphal tips and spores were grown three times on new media to ensure their purity. The isolates were stored in 15% glycerol at -80°C. The isolated fungus was identified microscopically by measuring conidia and conidiophores and was also examined morphologically through the culture's characteristics (**Zhu *et al.*, 2015**). The identification was confirmed using MALDI-TOF mass spectrometry (Bruker Biotyper), which analyzes ribosomal protein patterns to provide high accuracy (95 to 99%) and reliability for fungal identification (**Santos *et al.*, 2010**, **Singhal *et al.*, 2015**). Unlike traditional morphology-based methods, which can lead to misidentification, this method benefits from a large database (over 8,000 fungal spectra) and reproducibility (intra-assay variance less than 2%), allowing reliable species-level identification (**Normand *et al.*, 2017**). When compared to standard molecular techniques like ITS sequencing, the use of matrix-assisted laser desorption/ionization time-of-flight mass spectrometry (MALDI-TOF MS) for fungal strain identification provides significant advantages in speed and cost-effectiveness.

2.5. *In vitro* study of the effect of Se(IV) and SeNPs on fungal growth

Inhibition of hyphal growth was tested by agar dilution technique (**Wheat, 2001**) using four concentrations of Se(IV) and SeNPs, i.e. 50, 100, 150 and 200 ppm (Fig. 1). They were metered to warm PDA culture medium. Then small agar disc, originated from 7 days old pure culture of the fungus, was placed into the center of agar plates. Petri dishes were closed with Par film, and put into incubator at 25-28°C for 5 days. Two Petri-dishes were used for each treatment. Evaluation was carried out when the fungus overgrew the control agar plates. The growth of mycelium of treated plates was compared with that of control.

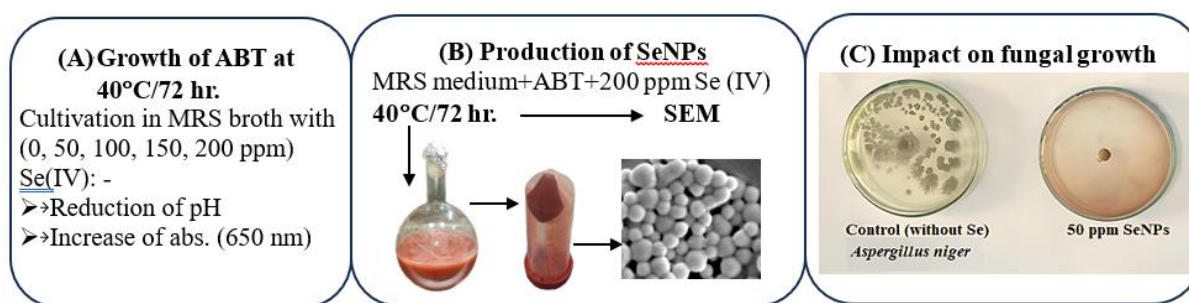


Fig. 1. Experimental flowchart.

Previous studies found that the minimum inhibitory concentrations (MICs) for Se(IV) range from 20 to 100 ppm against fungi such as *Candida albicans* and *Aspergillus spp.* Concentrations between 150 and 200 ppm can nearly completely inhibit growth (over 95%) (**Hosnedlova *et al.*, 2018**; **Zhang *et al.*, 2020**). Pilot trials indicated that 50 to 100 ppm reduced growth by 70 to 90%. Concentrations of 150 to 200 ppm improved effectiveness but approached toxicity levels for mammals (IC₅₀ around 250 ppm). Levels above 200 ppm could cause selenium to build up in the environment, which limits their use (**Kieliszek, 2019**). This range allows for comparisons with selenium nanoparticles (SeNPs), which are effective at lower doses (10 to 50 ppm) due to their higher bioavailability (**Wadhvani *et al.*, 2016**). For agricultural treatments, 50 ppm is suitable for preventive measures. 100 ppm is within food safety limits for coatings (EFSA: 0.15–0.3 mg/kg). 150 ppm is appropriate for medical

disinfectants, while 200 ppm can be used for immediate treatments like post-harvest fumigation. Se(IV) changes to insoluble Se^0 in soil, which lowers long-term toxicity. The 50 to 200 ppm range offers a balance of effectiveness, safety, and cost. It highlights the need for more research on the effects of different doses of Se(IV) on various fungi. Future improvements, such as nano-encapsulation or combined SeNP formulations, could lower effectively doses and encourage sustainability.

2.6. Mechanisms of SeNPs and Se(IV) as antifungal agents

2.6.1. Scanning Electron Microscopy (SEM)

Treated fungal samples were fixed in 2.5% glutaraldehyde, dehydrated in ethanol gradients (30–100%), and gold-coated for SEM analysis (JEOL JSM-6390). Images were captured at 10 kV to assess hyphal morphology, surface erosion, and nanoparticle adhesion. Untreated controls were processed identically (Zhang *et al.*, 2020).

2.6.2. Thiobarbituric acid reactive substances (TBARS) assay

The TBARS was measured at 532 nm absorbance as previously described Zommara *et al.*, (1995). with fungal-specific modifications made by Khatoon *et al.*, (2022).

2.7. Statistical analyses

Statistical analysis was conducted using the SPSS version 10.0 software (SPSS, 2016). Significant differences between means were assessed using Duncan's multiple range test at the significance level of $P \leq 0.05$. The data were expressed as mean \pm standard error (SE) of 3 replicates.

3. Results

3.1. Growth of LAB strains in MRS media

The LAB culture (LAB) growth profile was estimated by pursuing the increase of absorbance (Fig. 2) and reduction of pH (Fig. 3) in MRS media during 72 hr. of incubation at 37°C with different concentrations of Se(IV). The data illustrated in Fig. (2) tracks the absorbance at 650 nm of LAB culture, alone and in combination with varying concentrations of Se(IV) (50, 100, 150, and 200 ppm), over a 72-hour incubation period. The LAB culture without Se (control) shows a steady increase in absorbance from 0.105 at 0 hr. to 2.211 after 72 hr. of incubation. The growth curve exhibits a typical bacterial growth pattern. Slow initial growth Lag phase (0-4 hr.) (absorbance rises from 0.105 to 0.309). Rapid growth (4-12 hr.), with absorbance increasing sharply from 0.309 to 1.952 (Exponential phase). Stationary phase (12–72 hr.) with gradual rising of media absorbance from 1.952 to 2.211, indicating the culture is reaching a plateau.

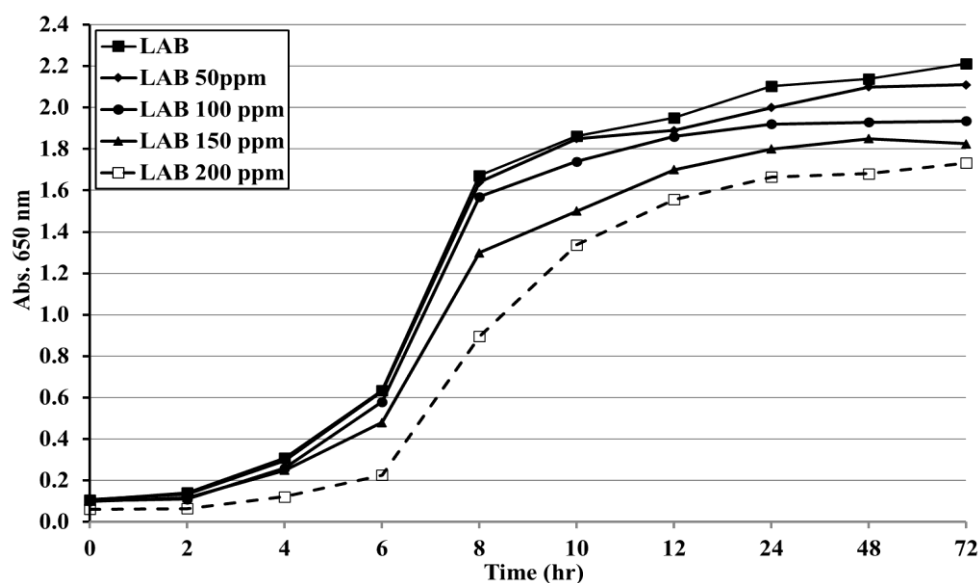


Fig. 2. Absorbance (650 nm) of MRS media supplemented with LAB and different concentrations (ppm) of Se(IV) during 72 hr. of incubation at 37°C.

On the other hand, all Se(IV) treated cultures (50–200 ppm) show a similar growth pattern but with progressively lower absorbance values as Se(IV) concentration increases. At 50 ppm of SeNPs, the growth curve is nearly identical to the control, with only slightly lower absorbance values (e.g., 2.211 vs. 2.110 at 72 hrs.). At 100 ppm of Se(IV), the absorbance is slightly lower than the control and 50 ppm treatment, reaching 1.935 at 72 hrs. The exponential phase is less pronounced (e.g., 1.860 vs. 1.952 for control at 12 hrs.). At higher Se(IV) concentration (150 ppm), the absorbance increased from 0.100 at 0 hr. to 1.825 at 72 hrs., noticeably lower than the control and lower concentrations (50–100 ppm). The exponential phase is less steep (e.g., 1.300 vs. 1.672 for control at 8 hrs.), and the stationary phase absorbance is consistently lower (1.800 vs. 2.103 for control at 24 hr.). At 200 ppm Se(IV), the absorbance was the lowest among all treatments, starting at 0.062 and reaching only 1.732 at 72 hrs. The lag phase is extended (0.122 vs. 0.309 for control at 4 hrs.), and the exponential phase is significantly delayed and less intense (0.896 at 8 hrs. vs. 1.672 for control).

The data illustrated in Fig. (3) tracks the pH of the MRS media. The pH reduction reflects acidification due to the ABT metabolism, primarily through lactic acid production.

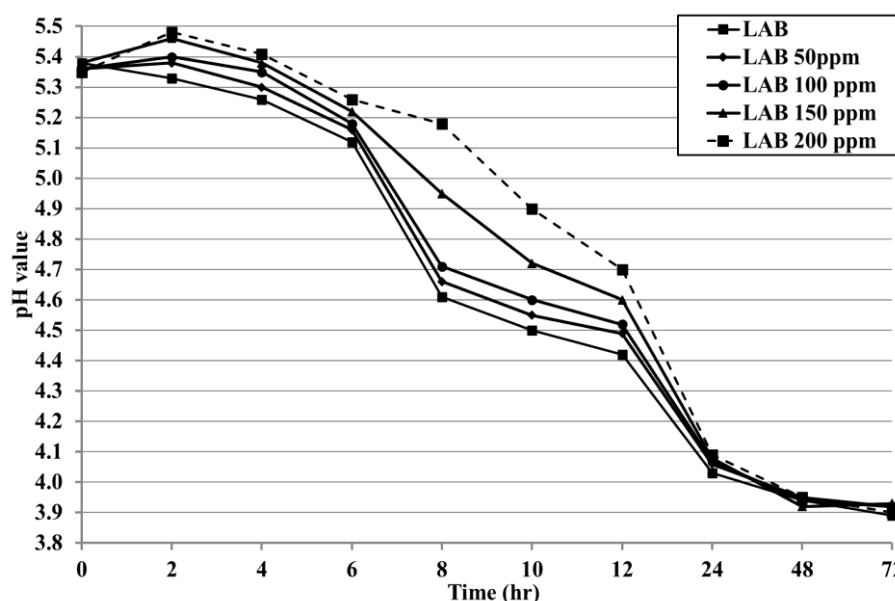


Fig. 3. Acidity development (pH) of MRS media supplemented with LAB and different concentrations (ppm) of Se(IV) during 72 hr. of incubation at 37°C.

The control showed steadily pH decrease from 5.38 at 0 hrs. to 3.89 at 72 hrs., reflecting typical LAB fermentation. The Lag phase (0–4 hrs.) showed slow pH decline (5.38 to 5.26), indicating initial metabolic adaptation. The Exponential phase (4–12 hrs) showed rapid pH drop (5.26 to 4.42), corresponding to peak lactic acid production during active growth. The Stationary phase (12–72 hrs.) showed gradual pH reduction (4.42 to 3.89), as metabolic activity slows but continues to produce acid. All Se(IV)-treated cultures show a similar acidification trend but with slower pH reduction at higher concentrations (150–200 ppm).

At 50 ppm, the pH decreases from 5.36 to 3.92 over 72 hrs., closely mirroring the control (3.89). The pH decline was nearly identical during the exponential phase (4.49 vs. 4.42 at 12 hrs. At 100 ppm, the pH dropped from 5.36 to 3.92, with slightly slower acidification during the exponential phase (4.52 vs. 4.42 at 12 hrs.). The final pH was equivalent to 50 ppm. At moderate concentration (150 ppm), the pH decreases from 5.38 to 3.93, but the decline is slower during the exponential phase (4.60 vs. 4.42 at 12 hrs.). The initial pH slightly increases to 5.46 at 2 hrs. At high concentration (200 ppm), The pH decreases from 5.35 to 3.90, but the acidification is notably slower for Se(IV) compared to control (5.41 vs. 5.26 at 4 hrs.; 4.70 vs. 4.42 at 12 hrs.). Therefore, Se(IV) at 200 ppm significantly hinders acid production. It is worth noting that, the media supplemented with Se(IV) resulted in gradual red color development in the media over the incubation period indicating the formation of SeNPs that reached its maximum level at the end of the incubation period.

3.2. Production of SeNPs

As shown in Fig. (4A) the cultivated MRS Medium was turned to dark red color after 72 hr. of incubation with Se(IV) and LAB culture as a result of the formation of SeNPs. The light microscope and TEM photo of the

produced SeNPs are shown in Fig. (4B and 4C), respectively. The photo showed spherical monoclinic crystals of SeNPs in different diameter size ranged from 45 nm-275 nm (Table 1). The EDX (Energy-Dispersive X-ray Spectroscopy) pattern of the obtained SeNPs is shown in Fig. (4C). It shows the elemental composition of a sample, likely selenium nanoparticles (SeNPs), based on the energy levels of X-rays emitted by the sample. There are prominent peaks labeled "Se" at around 1.4 keV and 11.2 keV, which correspond to the characteristic X-ray energies for Selenium (Se La and Se K α lines, respectively). The peaks labeled "Cu" at approximately 8 keV (Cu K α) and 8.9 keV (Cu K β) indicate the presence of Copper. A peak labeled "C" at around 0.3 keV (C K α) suggests the presence of carbon. No other significant peaks are labeled.

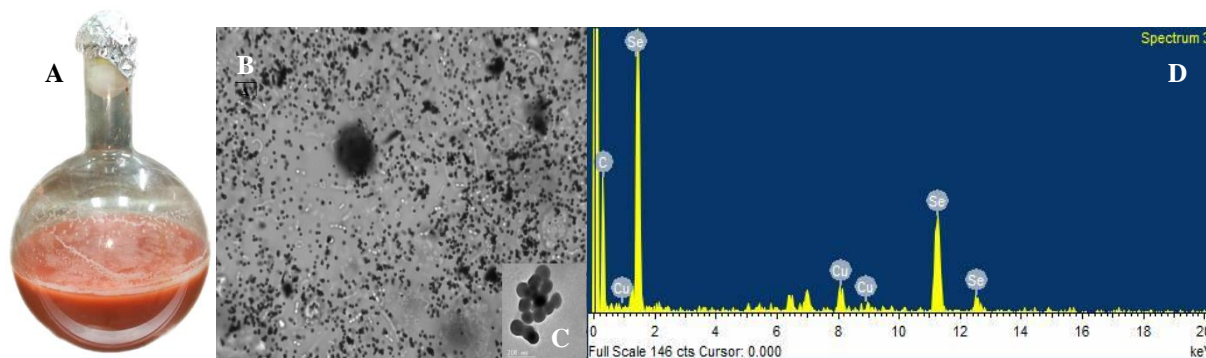


Fig. 4. SeNPs in MRS medium supplemented with 200 ppm Se(IV) (A), SeNPs photos by oil immersed lenses light microscope (B) and TEM (C) and EDX analysis of SeNPs (D).

3.3. Diameter size of SeNPs produced by the ABT culture cultivated in MRS media

Table (1) presents data on the diameter size (nm) of SeNPs produced by the ABT culture enumerated in MRS medium supplemented with different concentrations of selenite (Se(IV)) -50, 100, 150, and 200 ppm after 72 hr. of incubation at 40°C.

Table 1. Diameter size of SeNPs produced by LAB in MRS media supplemented with different concentrations of Se(IV) after 72hr. of incubation at 40°C.

Se(IV) concentration (ppm)	SeNPs Diameter size (nm)
50	45-275
100	47-256
150	65-244
200	50-250

The data in Table (1) demonstrated that, the smallest (45 nm) and the largest (275 nm) SeNPs are produced at 50 ppm. At 150 ppm, the size range is narrower (179 nm spread). Increasing Se(IV) concentration doesn't consistently increase or decrease the diameter range; the sizes fluctuate across concentrations. Also, the minimum diameter increases slightly with higher Se(IV) concentrations (from 45 nm at 50 ppm to 65 nm at 150 ppm), but this trend doesn't hold at 200 ppm (50 nm).

3.4. Antifungal effect of SeNPs and Se(IV) on different fungi strains

3.4.1. Effect on *Asp. Niger*

Data illustrated in Fig. (5) show the growth diameter (cm) of *Asp. niger* on PDA media supplemented with selenium nanoparticles (SeNPs) and selenite (SeIV) at concentrations of 50, 100, 150, and 200 ppm, compared to a control. The control group (no treatment) shows a growth diameter of 5.7 cm.

Addition of SeNPs decreased the fungal growth diameter from 2.0 cm (50 ppm) to 1.0 cm (150–200 ppm), showing dose-dependent inhibition with a threshold at 150 ppm. However, uniformly Se(IV) restricts growth to 1.0 cm across all concentrations.

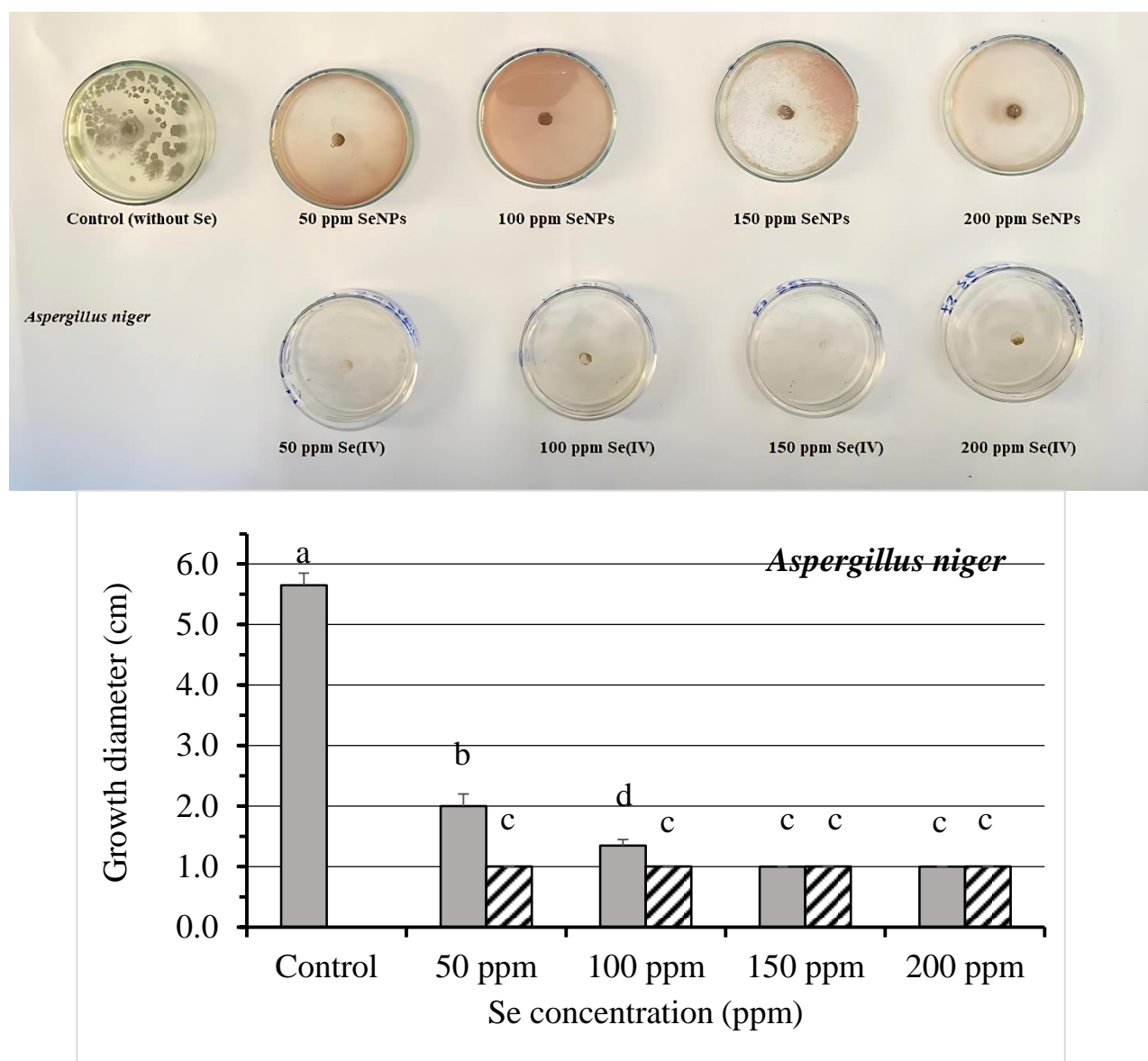


Fig. 5. Effect of different concentrations of SeNPs or Se(IV) on growth of *Asp. niger* cultivated on PDA media for 5 days at 28°C.

Data are mean \pm SE for 3 replicates

^{abcd} means with different superscripts letters are significantly different $P \leq 0.05$.

3.4.2. Effect on *Penicillium roqueforti*

The data presented in Fig. (6) show the effect of different concentrations (ppm) of SeNPs and Se(IV) on the growth diameter (cm) of *P. roqueforti*. The baseline growth diameter for the control group is 8.9 cm. At 50 ppm, the fungus maintains its normal growth with no noticeable effect of selenium in its ionic form (SeIV). On the other hand, SeNPs treatment reduced the growth diameter significantly to 1.3 cm. At higher concentrations (100, 150, and 200 ppm), Both of selenium forms completely inhibited growth across all concentrations (1.0 cm).

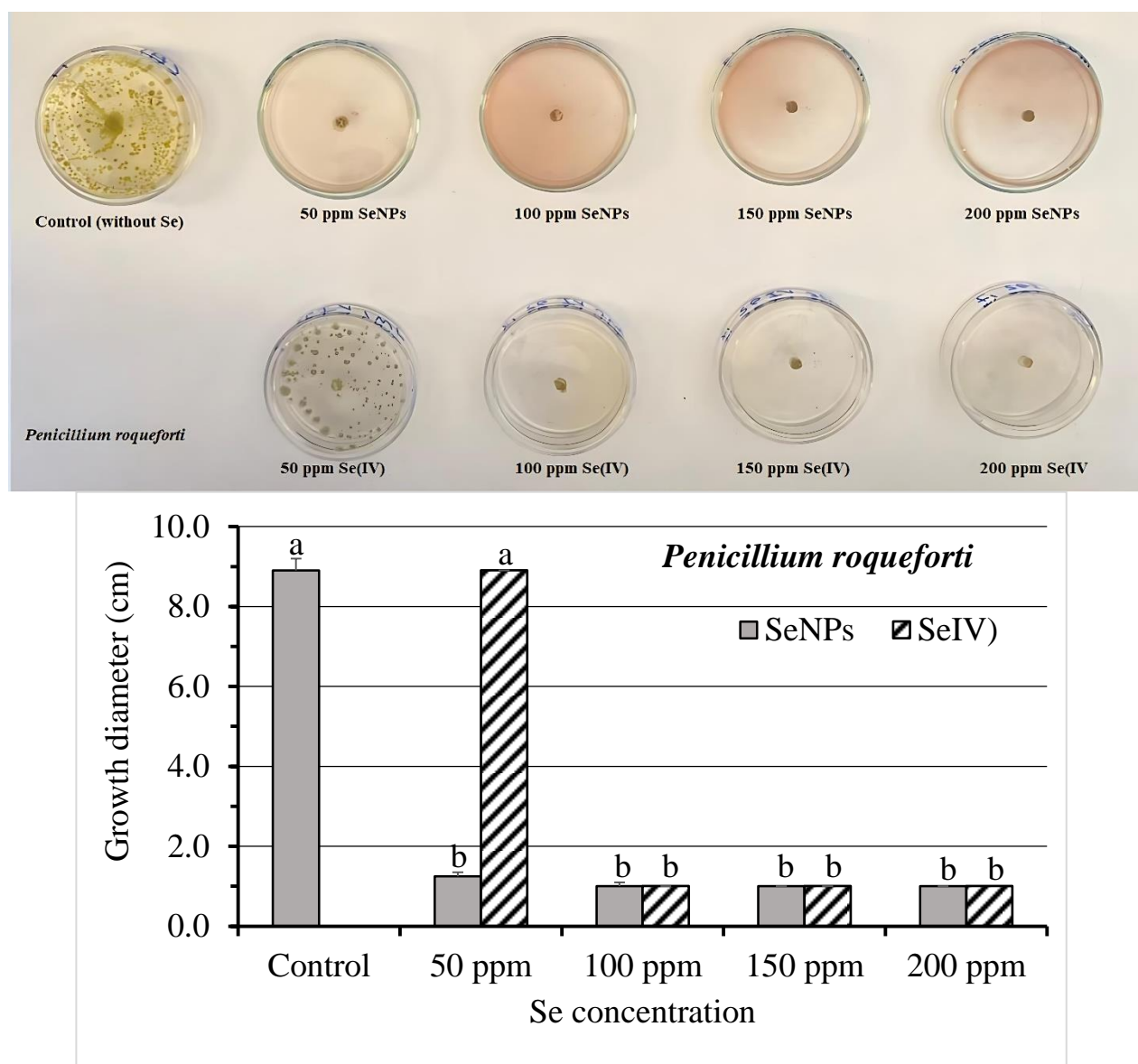


Fig. 6. Effect of different concentrations of SeNPs or Se(IV) on growth of *P. roqueforti* cultivated on PDA media for 5 days at 28°C.

Data are mean \pm SE for 3 replicates

^{ab} means with different superscripts letters are significantly different $P \leq 0.05$.

3.4.3. Effect on *Penicillium citrinum*

The data illustrated in Fig. (7) show the effect of different concentrations (ppm) of SeNPs and Se(IV) on the growth diameter (cm) of *P. citrinum*. Based on the provided data, the effect of the two types of selenium (SeNPs and SeIV) on the growth of *P. citrinum* demonstrates a distinct pattern in the ways that the various forms of selenium impact the growth of fungi. The baseline growth (control) diameter for the fungus is 5.7 cm. This serves as the normal growth measurement when no selenium treatment is applied. At 50 ppm, the growth diameter is reduced to 1.0 cm in both selenium forms (SeIV and SeNPs) treatments and remains at 1.0 cm at 100 ppm, 150 ppm, and 200 ppm.

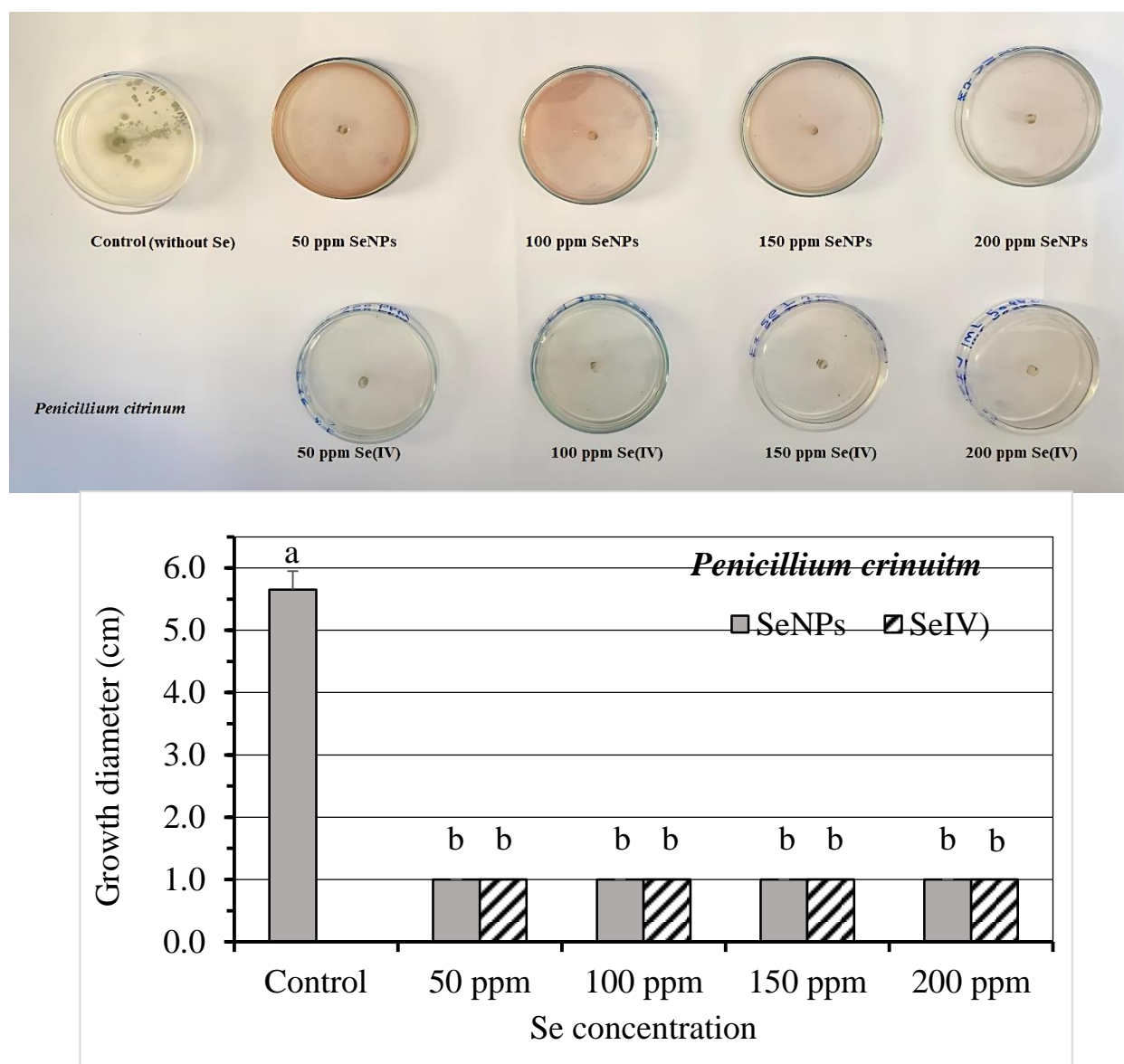


Fig. 7. Effect of different concentrations of SeNPs or Se(IV) on growth of *P. citrinum* cultivated on PDA media for 5 days at 28°C.

Data are mean \pm SE for 3 replicates

^{ab} means with different superscripts letters are significantly different $P \leq 0.05$.

3.4.4. Effect on *R. arrhizus*

The data presented in Fig (8). shows the growth diameter (cm) of *Rhizopus arrhizus*, a filamentous fungus, in the presence of selenium nanoparticle (SeNPs) and selenite (SeIV) at concentrations of 50, 100, 150, and 200 ppm, compared to a control (with no treatment). Growth diameter of control (9.0 cm reflects the optimal growth of *R. arrhizus* in the absence of selenium, serving as the baseline. Addition of 50 ppm SeNPs to the media resulted in a decrease of growth diameter to 3.6 cm, a ~60% reduction from the control, indicating moderate inhibition. Addition of 100 ppm, 150 ppm, and 200 ppm to the media reduced the growth diameter to 1.0 cm, an ~89% reduction, showing severe inhibition.

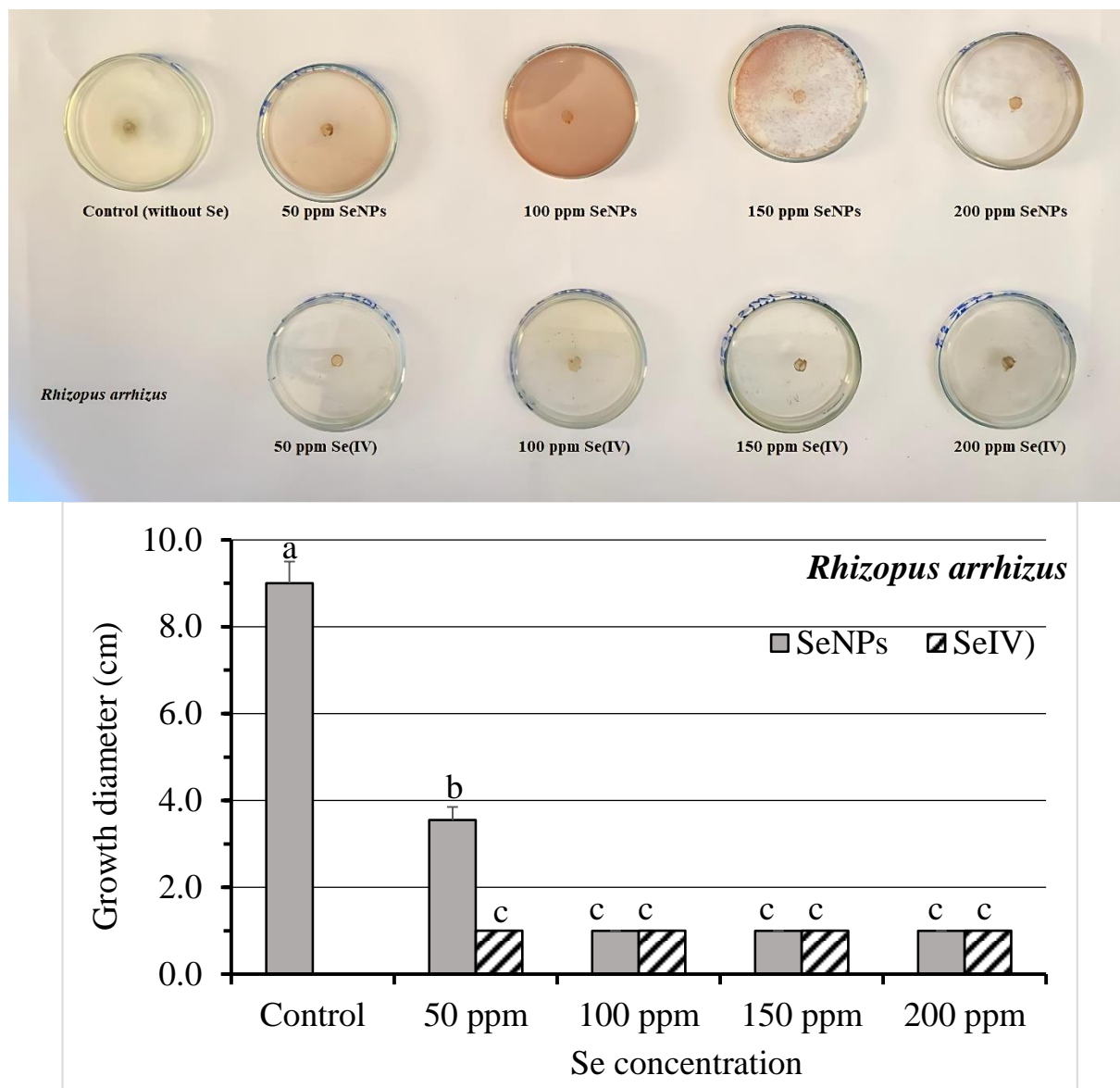


Fig. 8. Effect of different concentrations of SeNPs or Se(IV) on growth of *R. arrhizus* cultivated on PDA media for 5 days at 28°C.

Data are mean \pm SE for 3 replicates

^{abc} means with different superscripts letters are significantly different $P \leq 0.05$.

3.4.5. Effect on *Trichoderma spp*

The data illustrated in Fig. (9) show the effect of different concentrations (ppm) of SeNPs and Se(IV) on the growth diameter (cm) of *Trichoderma spp*. Based on the provided data, The fungus achieved a growth diameter of 3.9 cm. At 50 ppm, both forms of selenium (SeNPs or Se(IV)) significantly inhibited fungal growth, reducing the diameter to 1.4 cm (a ~64% reduction compared to the control) with no difference between SeNPs and Se(IV) at this concentration.

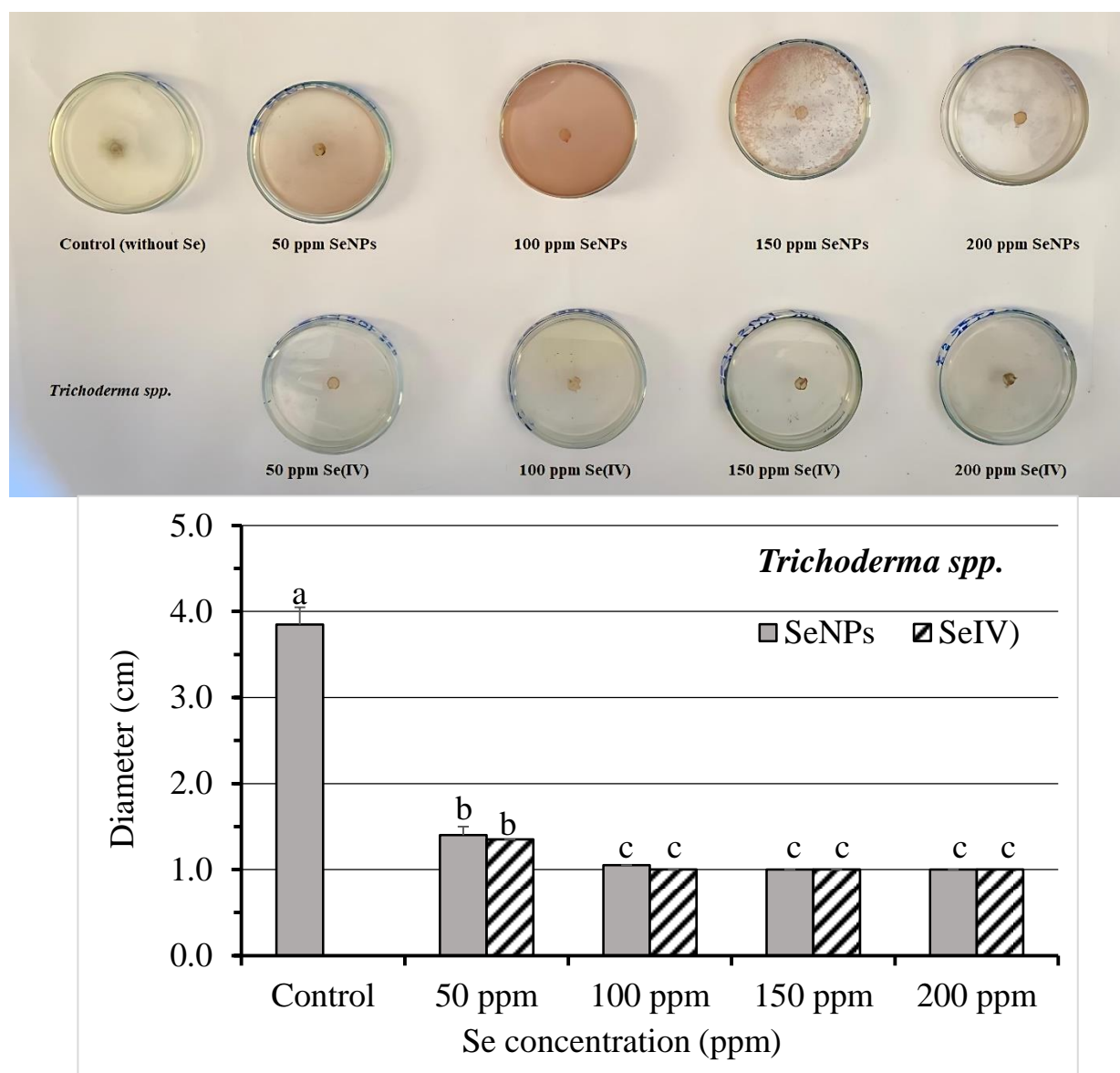


Fig. 9. Effect of different concentrations of SeNPs or Se(IV) on growth of *Trichoderma* spp. cultivated on PDA media for 5 days at 28°C.

Data are mean \pm SE for 3 replicates

^{abc} means with different superscripts letters are significantly different $P \leq 0.05$.

At 100 ppm SeNPs or SeIV, the growth inhibition increased further, with SeNPs restricting growth to 1.1 cm (~72% reduction) and slightly stronger inhibition to 1.0 cm (~74% reduction) by SeIV compared to SeNPs. No further inhibition was observed beyond 100 ppm for SeIV and 150 ppm for SeNPs. At higher concentrations (150 or 200 ppm), both SeNPs and SeIV completely restricted growth to 1.0 cm (~74% reduction).

4. Mechanisms of SeNPs and Se(IV) as antifungal agents

4.1. *Penicillium roqueforti*

The SEM images of *P. roqueforti* grown in PDA broth media supplemented with 200 ppm of Se(IV) or SeNPs and cultured at 25 °C for five days are displayed in Fig. (10). The control shows normal fungal morphology. It has intact, smooth hyphae with a uniform structure and no visible damage or deformities. Se(IV) displays severe structural damage with fragmented and collapsed hyphae. There is visible cellular content leakage and extensive surface pitting, indicating aggressive and rapid antifungal action. SeNPs shows moderate, targeted damage with surface roughening, partial collapse, and localized erosion without complete fragmentation. It maintains some structural integrity, suggesting gradual and controlled antifungal effects.

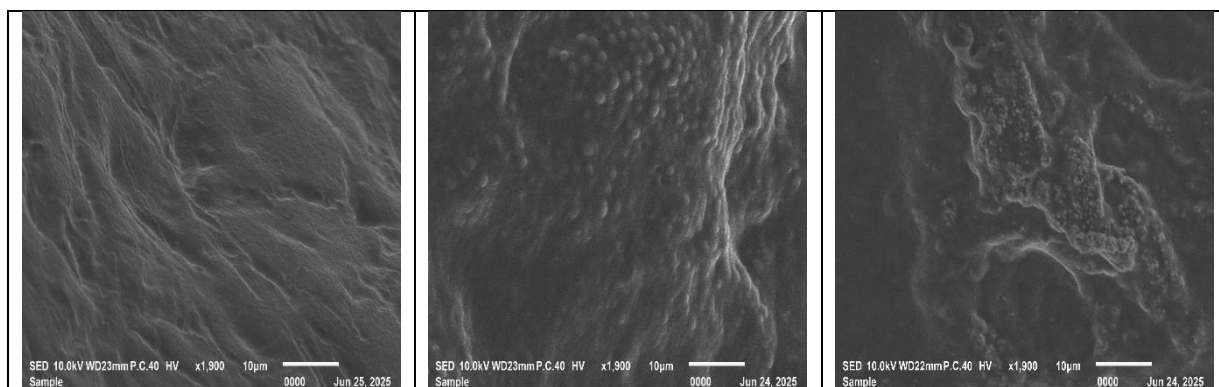


Fig. 10. SEM images showing the effect of 200 ppm of SeNPs or Se(IV) on *P. roqueforti* compared to control (untreated) after incubation in PDA broth medium for 5 days at 25 °C (1,900x).

4.2. *Penicillium citrinum*

The SEM images of *P. citrinum* grown in PDA broth media with 200 ppm of Se(IV) or SeNPs and cultured at 25 °C for five days are shown in Fig. (11). They reveal three different fungal shapes. The control sample, which is untreated, shows healthy, intact hyphae that have smooth surfaces and a uniform structure with no visible damage. This indicates normal fungal growth. Se(IV) shows severe structural damage. This is evident from complete hyphal fragmentation, leakage of cellular content, referred to as “ghost cells,” and extensive surface pitting. These signs suggest rapid and destructive antifungal action. In contrast, SeNPs show moderate, controlled damage. This is seen through roughened surfaces and partial collapse, with localized erosion but no complete breakdown. Some structural integrity remains, indicating gradual, targeted antifungal effects.

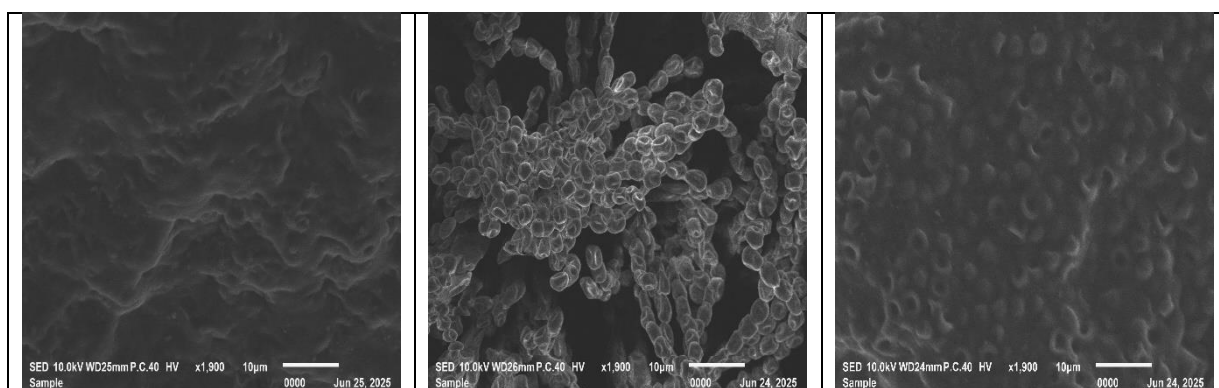


Fig. 11. SEM images showing the effect of 200 ppm of SeNPs or Se(IV) on *P. citrinum* compared to control (untreated) after incubation in PDA broth medium for 5 days at 25 °C (1,900x).

4.3. *Asp. niger*

The SEM images of *Asp. niger* grown on PDA broth media supplemented with 200 ppm of Se(IV) or SeNPs and incubated for five days at 25 °C are displayed in Fig. (12). The control shows intact, smooth hyphae with a uniform structure and no visible damage, indicating healthy fungal growth. Se(IV) exhibits severe structural damage, including fragmented and collapsed hyphae, cellular leakage (“ghost cells”), and surface porosity. This may show rapid and aggressive antifungal action through thiol group inactivation and oxidative stress. SeNPs display moderate targeted damage, with surface roughening, partial hyphal shrinkage, and localized erosion without complete fragmentation. This may demonstrate gradual and controlled antifungal effects through ROS generation and physical disruption.

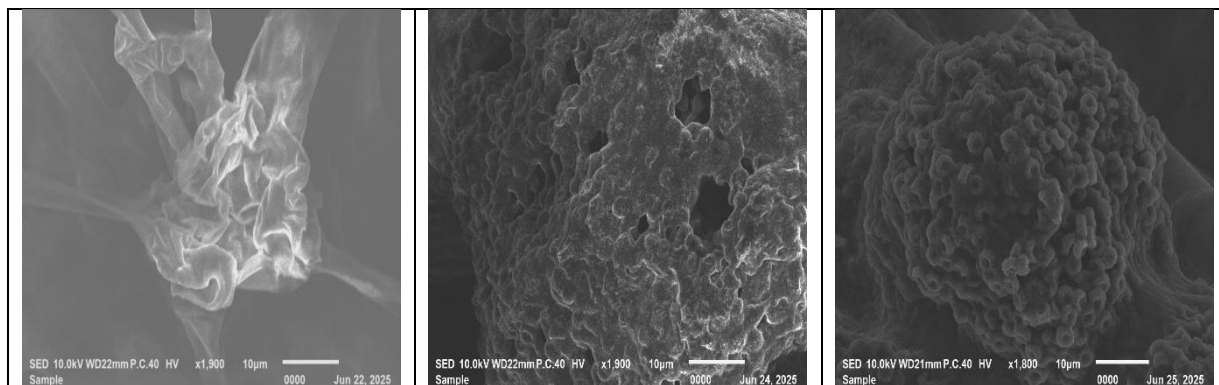


Fig. 12. SEM images showing the effect of 200 ppm of SeNPs or Se(IV) on *Asp. niger* compared to control (untreated) after incubation in PDA broth medium for 5 days at 25 °C (1,900x).

4.4. *R. arrhizus*

The comparative SEM image analysis of *R. arrhizus* morphology in control and Se treated samples is presented in Fig. (13). The Control (Untreated) shows pristine, healthy hyphae with smooth surfaces and a consistent cylindrical structure throughout. There is no visible damage or deformities, which represents the baseline fungal architecture. Se(IV) leads to complete structural collapse of hyphae, extensive fragmentation, and cellular leakage, with the surface appearing corroded and showing multiple rupture points. These findings indicate rapid and non-selective destruction. SeNPs display moderate surface erosion and pitting, along with partial shrinkage of hyphal structures and localized damage, while still maintaining overall continuity. This suggests a controlled, targeted antifungal action.

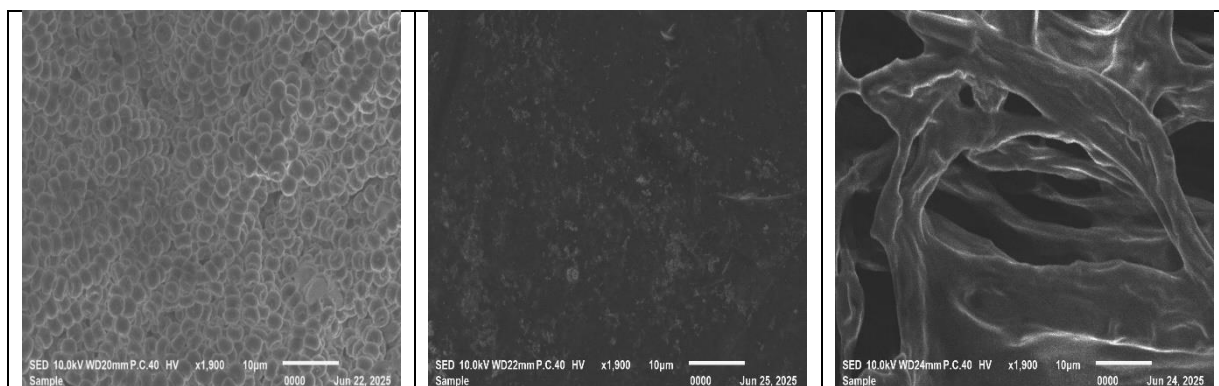


Fig. 13. SEM images showing the effect of 200 ppm of SeNPs or Se(IV) on *R. arrhizus* compared to control (untreated) after incubation in PDA broth medium for 5 days at 25 °C (1,900x).

4.5. *Trichoderma spp.*

The *Trichoderma spp.* SEM images show three distinct shapes that illustrate how different Se treatments affect fungal structures are shown in Fig. (14). The control sample has healthy, intact hyphae with smooth surfaces and a uniform cylindrical shape. There is no visible damage or deformities, representing the baseline fungal architecture. The Se(IV) treated sample shows total structural collapse, with fragmented and "melted" hyphae and significant cellular content leakage. This indicates rapid, non-selective destruction. The SeNPs treated sample displays moderate surface erosion and partial shrinkage of hyphal structures while still maintaining overall structural continuity. This suggests controlled, targeted damage. Thus, these findings rank damage severity as follows: Se(IV) > SeNPs > control, and structural integrity as control > SeNPs > Se(IV).

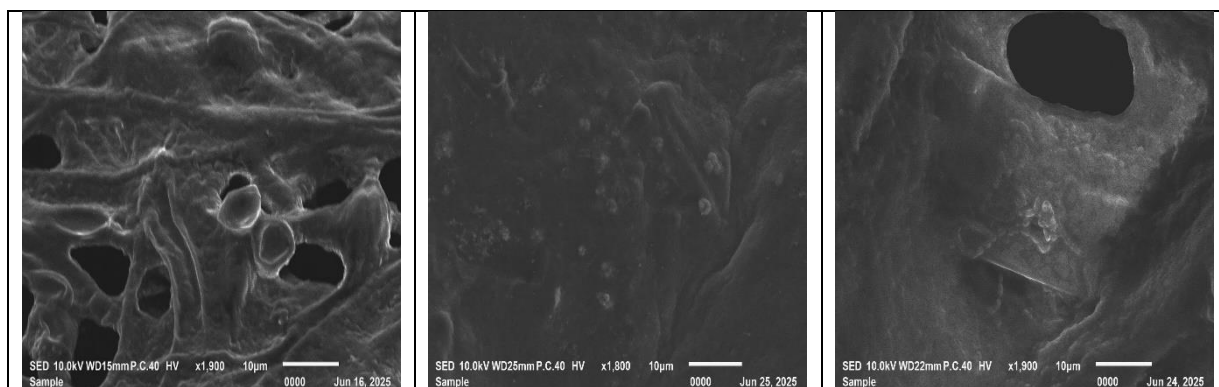
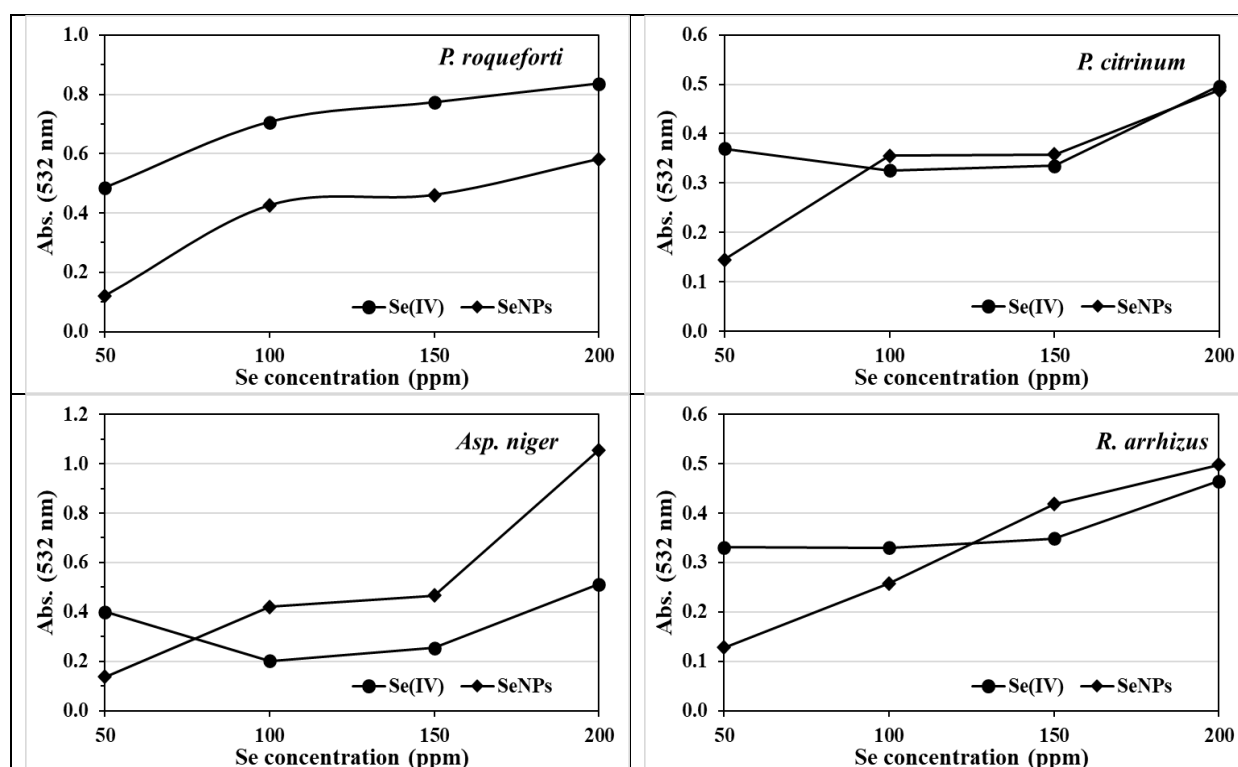


Fig. 14. SEM images showing the effect of 200 ppm of SeNPs or Se(IV) on *Trichoderma spp.* compared to control (untreated) after incubation in PDA broth medium for 5 days at 25 °C (1,800x -1,900x).

5. TBARS Analysis in Five Fungi Strains at 200 ppm Se(IV) and SeNPs

The thiobarbituric acid reactive substances (TBARS) assay measures lipid peroxidation in five fungi strains: *P. roqueforti*, *P. citrinum*, *Asp. niger*, *R. arrhizus*, and *Trichoderma spp.* This is done under 200 ppm treatment with selenium (Se) as Se(IV) or SeNPs, as shown in Fig. 15. The data show different responses across strains, reflecting variations in oxidative stress and Se interaction. At 200 ppm, *P. roqueforti* had the highest TBARS absorbance for Se(IV) at 0.836 among all strains, which indicates significant lipid peroxidation. Its response to SeNPs was lower at 0.582. Likewise, *P. citrinum* had similar TBARS values for Se(IV) at 0.496 and SeNPs at 0.488. *Asp. niger* showed a significant difference, with SeNPs resulting in a much higher TBARS value of 1.055 compared to Se(IV) at 0.512. *R. arrhizus* had moderate TBARS values, with Se(IV) at 0.465 and SeNPs at 0.498. *Trichoderma spp.* showed similar trends, with Se(IV) at 0.467 and SeNPs at 0.483. This indicates comparable oxidative stress responses.



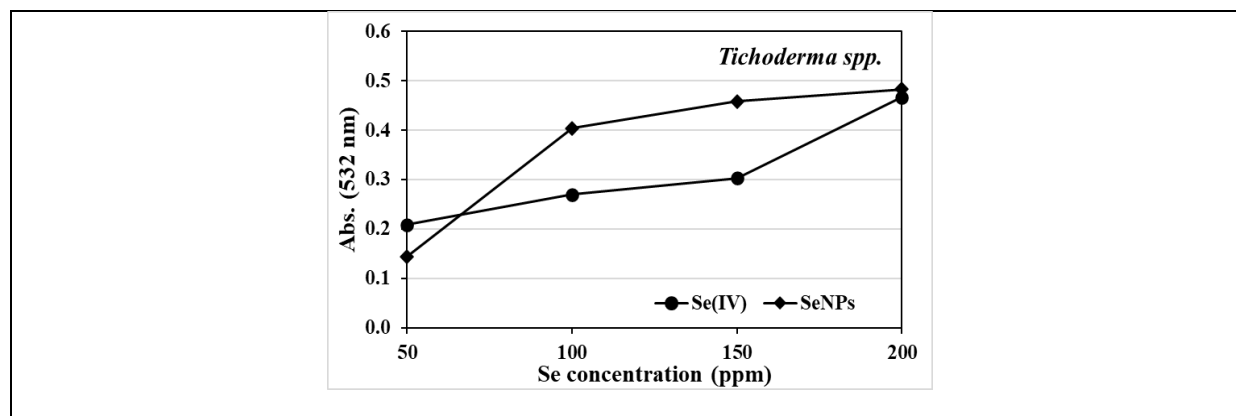


Fig. 15. Lipid peroxidation (TBARS) in five fungal strains treated with 200 ppm of either SeIV or SeNPs.

6. Discussion

6.1. Growth of LAB strains in MRS media

The antifungal properties of selenium nanoparticles (SeNPs) make them a viable substitute for conventional techniques. Using Se-resistant bacteria for SeNPs biosynthesis is an economical and sustainable method. In the present study, the ABT culture was used for SeNPs biosynthesis from Se(IV). The impact of different concentration (ppm) of Se(IV) on the viability of the ABT culture and its ability for SeNPs biosynthesis was estimated in MRS medium by measuring the increase of media absorbance (650 nm) and reduction of pH for 72 hr at 40°C. The absorbance data illustrated in Fig. (2) showed that, at 50 ppm of Se(IV), the growth curve was nearly identical to the control, with only slightly lower absorbance values (e.g., 2.211 vs. 2.110 at 72 hrs.). This indicates that 50 ppm Se(IV) has minimal impact on ABT culture growth. At 100 ppm of Se(IV), the absorbance was slightly lower than the control and 50 ppm treatment while the exponential phase was less pronounced, suggesting a mild inhibitory effect, meanwhile 150 ppm Se(IV) exert a moderate inhibitory effect. Supplementation the medium with 200 ppm SeNPs resulted in a strong inhibitory effect.

Same trend was found regarding the media pH values during the incubation period. At 50 ppm, the pH to 3.92 over 72 hrs., closely mirroring the control (3.89). The pH decline was nearly identical during the exponential phase (4.49 vs. 4.42 at 12 hrs.), indicating minimal interference with acid production. At 100 ppm, the pH dropped to 3.92, with slightly slower acidification during the exponential phase (4.52 vs. 4.42 at 12 hrs.). The final pH was equivalent to 50 ppm, suggesting comparable metabolic activity by 72 hrs. These data indicate that, low SeNPs concentrations (50–100 ppm) have negligible effects on the ABT culture acid production, likely due to tolerance or incorporation of selenium into metabolism without significant toxicity. At moderate concentration (150 ppm), the pH decreased to 3.93, but the decline is slower during the exponential phase (4.60 vs. 4.42 at 12 hrs.). The initial pH slightly increased to 5.46 at 2 hrs., possibly due to SeNPs interactions with media components or delayed ABT culture metabolism. At high concentration (200 ppm), The pH decreased to 3.90, but the acidification was notably slower for SeNPs compared to control (5.41 vs. 5.26 at 4 hrs.; 4.70 vs. 4.42 at 12 hrs.). Therefore, SeNPs at 200 ppm significantly interferes with the acid production, likely due to toxicity affecting the ABT culture growth and metabolism, that consistent with reduced absorbance (1.732 vs. 2.211 at 72 hrs.).

The previous results (Fig. 2 and 3) demonstrated that, low SeNPs concentrations (50–100 ppm) do not inhibit the ABT culture growth, possibly indicating tolerance or even potential incorporation of selenium into bacterial metabolism without toxicity. At 150 ppm, Se(IV) exerts a moderate inhibitory effect reducing growth rate and final cell density. However, at 200 ppm Se(IV) has a strong inhibitory effect, likely due to toxicity. The obtained data are in accordance with our previous findings (Zommara *et al.*, 2018, 2020, 2021, 2022). Considering the gradual formation of SeNPs in the medium in direct proportion to the increase in incubation time, the previous effects, whether the increase in absorbance or the decrease in acidity, can be attributed to the effect of both types of selenium (SeIV or SeNPs) on the bacterial culture. The antimicrobial effects of (SeNPs) are mediated by a number of mechanisms, i.e. the rupture of cell membranes, the production of reactive oxygen species (ROS), and disruption of cellular functions (Wang *et al.*, 2017, Blinova *et al.*, 2023), leading to reduced growth, suggesting a dose-dependent effect of SeNPs on bacterial growth.

SeNPs' effect on LAB is important for probiotic use, and it depends on the dose. At low levels, less than 50 ppm, SeNPs increase the growth of *Lactobacillus spp.* by 20 to 30%. They also raise selenium bioaccumulation, which

boosts the antioxidant capacity of probiotics, such as achieving 79.2% DPPH scavenging at 100 μ M (Kieliszek *et al.*, 2015). However, at 100 to 200 ppm, SeNPs decrease LAB viability by 15 to 40%. This decline may be caused by ROS-mediated membrane stress, which limits their application in fermented foods like yogurt (Shakibaie *et al.*, 2015). Therefore, it is suggested that SeNPs in probiotic applications should be limited to 25 to 50 ppm. This balance helps maintain antifungal effectiveness while preserving LAB, making them suitable for functional foods and gut health products.

6.2. Production of SeNPs

As shown in Fig. (4A) the cultivated MRS Medium was turned to dark red color after 72 hr. of incubation with Se(IV) and LAB culture as a result of the formation of SeNPs. The EDX (Energy-Dispersive X-ray Spectroscopy) pattern (Fig. 4D) of the obtained SeNPs (Fig. 4C) shows the elemental composition of a sample. There are prominent peaks labeled "Se" at around which correspond to selenium. This confirms the presence of selenium, consistent with SeNPs. The peaks labeled "Cu" indicate the presence of copper from the sample itself, a substrate, or a TEM grid commonly used in nanoparticle analysis. A peak labeled "C" suggests the presence of carbon, which is often seen in EDX spectra due to carbon coating, organic ligands, or contamination. No other significant peaks are labeled, indicating that the sample is relatively pure in terms of major elemental composition, aside from Se, Cu, and C. The spectrum shows a good signal-to-noise ratio for the Se peaks, suggesting a decent concentration of selenium in the sample. Therefore, the EDX chart confirms that the sample contains selenium, supporting the presence of SeNPs. The copper and carbon signals are likely from the sample preparation (e.g., a copper grid or carbon coating) rather than the nanoparticles themselves. The biological production of SeNPs by ABT culture presents a new way to obtain selenium dietary supplements. SeNPs may be able to offer the health benefits of selenium in a form that is easily ingested (Zommara *et al.*, 2018, Salama *et al.*, 2021).

6.3. Diameter size of SeNPs produced by ABT culture

MRS medium is widely used for the selective enumeration of lactic acid bacteria (LAB), including the ABT culture commonly found in fermented dairy products like yoghurt. (Dave & Shah, 1996). As presented in Table (1), the used culture can reduce Se(IV) to SeNPs across all tested concentrations. There is no clear linear trend in size variation with increasing Se(IV) concentration, indicating that concentration may not be the sole factor influencing nanoparticle size. The diameter size of selenium nanoparticles (SeNPs) produced by lactic acid bacteria (LAB) cultures can vary depending on multiple factors such as the specific used LAB strain, culture conditions (pH, temperature, selenium precursor concentration), growth phase when selenium is introduced and duration of incubation. There were no direct studies using the ABT culture for SeNPs production, but a few papers have explored selenium enrichment in ABT-based probiotic yoghurts or dairy matrices. Moreno-Martin *et al.*, (2017) synthesized SeNPs using *L. acidophilus*, *L. delbrueckii* subsp. *bulgaricus*, and *L. reuteri*. Transmission electron microscopy revealed stable, predominantly monodispersed, and spherical SeNPs with an average size of 146 ± 71 nm. Dynamic light scattering and nanoparticle tracking analysis indicated hydrodynamic sizes of 258 ± 4 nm and 187 ± 56 nm, respectively. Lei *et al.*, (2024) utilized *L. acidophilus* HN23 to reduce sodium selenite into SeNPs. The resulting SeNPs were spherical, with sizes ranging from 60 to 300 nm, and comprised approximately 65.8% elemental selenium. Prokisch and Zommara (2011) examined the ability of several LAB of the following species; *L. bulgaricus*, *L. acidophilus*, *Bif. bifidum*, *S. thermophilus*, *L. casei*, *L. rhamnosus* and *Bif. Longum* for SeNPs production. They found that, selenium comprising 400-500 nm sized nanospheres is produced by *Bif. bifidum* or *Bif. longum*. The genus *Lactobacillus*, produces selenium nanospheres comprising 100-300 nm. However, *S. thermophilus* produced 50-100 nm sized nanospheres. Also, Krausova *et al.*, (2021) evaluated the *in vivo* bioavailability of selenium in selenium-enriched *S. thermophilus*. They found that, the SeNPs produced had sizes ranging from 60 to 280 nm.

6.4. Antifungal effect of SeNPs and Se(IV) on different fungi strains

6.4.1. Effect on *Asp. niger*

Data presented in Fig. (4) show the growth diameter (cm) of *Asp. niger* on PDA media supplemented with selenium nanoparticles (SeNPs) and selenite (SeIV). The control group (no Se treatment) shows a growth diameter of 5.7 cm, indicating unrestricted fungal growth under standard conditions. Addition of SeNPs showed dose-dependent inhibition with a threshold at 150 ppm. However, uniformly Se(IV) restricts growth to 1.0 cm across all concentrations, indicating stronger antifungal potency even at 50 ppm. These results indicate that SeIV is more effective to suppress growth of *Asp. niger* at 50 ppm (1.0 cm vs. 2.0 cm for SeNPs), but both achieve similar inhibition (1.0 cm) at higher concentrations. The antifungal effect of SeNPs and SeIV against *Asp.*

niger likely involves multiple mechanisms (Cairns *et al.*, 2018, Kazempour *et al.*, 2020). SeIV may generate reactive oxygen species (ROS) (e.g., superoxide radicals, hydrogen peroxide) faster than SeNPs, explaining its immediate maximal inhibition even at 50 ppm. Also, it may directly inhibit spore germination that preventing the spread of fungal growth over a wider area. The dose-dependent effect of SeNPs (up to 100 ppm) suggests gradual membrane damage, while SeIV acts instantly. Based on the available search results, there's no direct evidence to support the claim that SeIV is effective at suppressing the growth of *Asp. niger*. However, there is conflicting evidence about the antifungal effect of selenium nanoparticles (SeNPs), with some studies suggesting that SeNPs can stimulate the growth of specific fungi, such as *Asp. niger*, in a dose-dependent way (Moglad *et al.*, 2023, Schuster *et al.*, 2024). Microscopic investigations have verified their potent antifungal and antispore properties (Islam *et al.*, 2022). *Asp. niger* development is complicatedly affected by SeNPs, and results may differ depending on concentration and particular experimental condition (Bafana *et al.*, 2018, Kazempour *et al.*, 2020).

6.4.2. Effect on *Penicillium roqueforti*

As shown in Fig. (5), the baseline growth diameter for the control indicates normal growth conditions for the fungus. At 50 ppm, no noticeable effect of selenium in its ionic form (SeIV) however, SeNPs treatment reduced the growth diameter significantly indicating a strong inhibitory effect of SeNPs on *P. roqueforti* growth at this concentration. At higher concentrations, both of selenium forms completely inhibited growth across all concentrations suggesting highly toxic effect at concentrations as low as 100 ppm. These findings indicated that, SeNPs appear more effective at lower concentrations (50 ppm) than Se(IV) for inhibiting *P. roqueforti* growth, which could be due to the nanoparticles' higher reactivity or bioavailability. At 100 ppm and above, both forms are equally effective, likely because the selenium concentration reaches a saturation point for toxicity to the fungus. Currently, there is limited direct evidence from the available data specifically addressing the effectiveness of SeNPs in suppressing the growth of *P. roqueforti*. The lack of concrete evidence for *P. roqueforti* implies that although SeNPs exhibit potential antifungal properties (Devi *et al.*, 2023), the mentioned literature has not confirmed their efficacy against this particular species, which is frequently employed in the manufacturing of blue cheese. Given that *P. roqueforti* is appreciated in food production rather than being suppressed, which can point to a gap in the literature. Therefore, any inhibitory effects must be confirmed by more research. Wang *et al.*, (2016) examined the effects of selenium on *P. expansum*, including forms of selenium Se(IV) such as sodium selenite. The results demonstrated a considerable suppression of spore germination, germ tube elongation, and mycelial spread in culture media. Because *Penicillium* species share physiological characteristics, it is possible that Se(IV) will have similar inhibitory effects on other species, including *P. roqueforti*.

6.4.3. Effect on *Penicillium citrinum*

Based on the provided data (Fig. 6), the effect of selenite ions (SeIV) and SeNPs on the growth of *P. citrinum* shows a clear trend in how the different forms of selenium affect fungal growth. The baseline growth (control) serves as the normal growth measurement when no selenium treatment is applied. The reduction of fungi growth at 50 ppm indicates a strong inhibitory effect on fungal growth starting from the lowest concentration and continuing at higher concentrations (200 ppm). This suggests that both forms of Se are highly toxic as evidenced by the complete inhibition of the fungal growth in a dose-independent manner, meaning that increasing the concentration above 50 ppm does not further reduce growth inhibition (perhaps because the effect has reached its maximum toxicity). Studies on *P. citrinum* itself often focus on its growth conditions and mycotoxin production (e.g., citrinin), however, there is no specific study cited that directly tested Se(IV) or SeNPs against *P. citrinum*. However, we must take into account that SeNPs has antifungal effect through different mechanisms that are likely to affect *P. citrinum* in the same way (Wang *et al.*, 2016, El-Saadony *et al.*, 2021, Devi *et al.*, 2023, Nile *et al.*, 2023, Serov *et al.*, 2023).

6.4.4. Effect on *R. arrhizus*

As illustrated in Fig (7), growth diameter of control reflects the optimal growth of *R. arrhizus* in the absence of selenium, serving as the baseline. Supplementation the medium with 50 ppm SeNPs reduced the growth diameter by about 60% compared to the control, indicating moderate inhibition. Increasing the SeNPs to 200 ppm in the media resulted in severe growth inhibition by about 89%. These results demonstrate a dose-dependent inhibitory effect for SeNPs up to 100 ppm, beyond which additional concentrations do not further reduce growth, suggesting a saturation point for toxicity. On the other hand, the growth diameter of *R. arrhizus* on SeIV treated media at all concentrations was similar (1.0 cm), indicating complete inhibition (about 89% reduction from control) even at the lowest dose (50 ppm). Therefore, these data suggest that SeIV has strong inhibitory effect at

all tested concentrations, with no dose-dependent variation, indicating maximum toxicity is achieved at or below 50 ppm. When comparing the effect of SeNPs vs. SeIV we can conclude that, at 50 ppm, SeNPs (3.6 cm) allow significantly more growth than SeIV (1.0 cm), indicating that SeNPs are less toxic to *R. arrhizus* at lower concentrations. However, at 100 ppm and above, both treatments reduce growth to 1.0 cm, suggesting equivalent inhibitory effects at higher doses. SeIV has more potent toxicity than SeNPs at lower concentrations, while the larger particle size or slower release of SeNPs may moderate their effect at 50 ppm.

R. arrhizus is a fast-growing, opportunistic fungus often studied in bioremediation (Fourest *et al.*, 1994), industrial fermentation (Zhao, and Chen 2019, Zhang *et al.*, 2020), or as a plant pathogen. Its sensitivity to selenium suggests potential applications in controlling fungal contamination or growth in agricultural and industry. stronger effect of SeIV may stem from its rapid uptake and conversion to reactive selenium species, while SeNPs may act more slowly via surface interactions or gradual selenium release. The plateau at 1.0 cm for both treatments at higher concentrations suggests a minimum viable growth diameter, possibly reflecting a small, stressed colony or experimental measurement limits. There may be a research gap in the absence of specific studies that examined the effect of SeIV or SeNPs directly against *R. arrhizus*, as the organism is more frequently examined for its beneficial function (bioremediation and industrial fermentation). Although SeNPs' broad-spectrum antifungal potential is frequently emphasized in the conventional narrative, claims of efficacy should be viewed seriously in the absence of direct proof for *R. arrhizus*.

6.4.5. Effect on *Trichoderma* spp.

Based on the provided data illustrated in Fig. (8), the effect of of SeNPs and Se(IV) on the growth of *Trichoderma* spp. indicated normal growth in the absence of selenium (control). At 50 ppm, both of SeNPs or SeIV significantly inhibited the fungal growth by about 64% compared to the control. Increasing the concentrations to 100 ppm up to 200 ppm increased the inhibition to about 72% and 74% for SeNPs and Se(IV), respectively. These data indicated that, both Se forms significantly inhibit *Trichoderma* spp. growth in a dose-dependent manner. Unfortunately, there is no direct studies address the effect of SeIV or SeNPs on suppressing *Trichoderma* growth. Most research focuses on *Trichoderma*-synthesized SeNPs for biocontrol of other fungi (Nandini *et al.*, 2017, Samer *et al.*, 2024, Voloshchuk *et al.*, 2024).

Although, SeIV may be marginally more effective at intermediate concentrations, SeNPs (often considered safer) show comparable effects at higher doses. This high bioavailability allows selenite to interact more extensively with cellular components, increasing its toxic potential at lower doses compared to SeNPs, which have a more controlled release and lower solubility (Hosnedlova *et al.*, 2018). Xu, C. (2020) suggested that in safety evaluation based on cell and animal models, the toxicity of Se species is ranked as follows: selenate > selenite > selenomethionine > SeNPs. The high bioavailability of selenite to interact more extensively with cellular components, increasing its toxic potential at lower doses compared to SeNPs, which have a more controlled release and lower solubility (Sampath *et al.*, 2024).

SeNPs and Se(IV) have strong antifungal effects against *P. roqueforti*, *P. citrinum*, *Asp. niger*, *R. arrhizus*, and *Trichoderma* spp. However, their strain-specific mechanisms, the effects of SeNP size, and their impact on beneficial microbes like lactic acid bacteria (LAB) are not well studied. This research uses scanning electron microscopy (SEM), thiobarbituric acid reactive substances (TBARS) assays, and MALDI-TOF to explore these factors at concentrations of 50–200 ppm. The findings will help in applications related to food safety, healthcare, agriculture, and probiotics.

SEM reveals significant hyphal fragmentation in *P. roqueforti* (TBARS: 0.582 Abs) and almost complete disintegration in *A. niger* (TBARS: 1.055 Abs) at 200 ppm. This effect results from ergosterol binding and nanoparticle adhesion, similar to the action of polyenes but with lower toxicity (Wadhwani *et al.*, 2016). The size of the SeNPs (45–275 nm) plays a crucial role in their effectiveness, smaller particles (45–100 nm) improve cellular uptake and reactive oxygen species (ROS) production. This leads to a 20–30% increase in antifungal activity compared to larger particles (150–275 nm), which mainly cause physical damage but penetrate less effectively (Shakibaie *et al.*, 2015). SeIV inactivates thiol groups and causes DNA breaks (Zhang *et al.*, 2020; Hosnedlova *et al.*, 2018). SEM shows pitting in *P. citrinum* (TBARS: 0.496 Abs) and corrosion in *R. arrhizus* (TBARS: 0.465 Abs). *Trichoderma* spp. displays resilience (TBARS: 0.467 for SeIV vs. 0.483 for SeNPs).

In agriculture, SeNPs inhibit *Fusarium oxysporum* at 50–100 µg/mL, leading to a 96% reduction in rot (Vahdati & Moghadam, 2020). For probiotic uses, SeNPs at concentrations below 50 ppm promote *Lactobacillus* spp. growth by 20–30% and enhance selenium bioaccumulation. This boosts antioxidant capacity, achieving 79.2% DPPH scavenging at 100 µM. However, concentrations of 100–200 ppm decrease LAB viability by 15–40% due

to ROS stress. This suggests a range of 25–50 ppm is preferable for functional foods (Kieliszek *et al.*, 2015). Smaller SeNPs (45–100 nm) are less toxic to LAB because they aggregate less, making them more compatible with probiotics.

7. Mechanisms of SeNPs and Se(IV) as antifungal agents

7.1. Integrated Analysis of SEM and TBARS Data on Selenium Effects in Fungal Strains

The antifungal effects of 200 ppm selenite (SeIV) and selenium nanoparticles (SeNPs) on five fungal strains, *P. roqueforti*, *P. citrinum*, *Asp. niger*, *R. arrhizus*, and *Trichoderma spp.*, were investigated using scanning electron microscopy (SEM) and TBARS assays. These complementary methods show strain-specific structural damage and oxidative stress, highlighting the different effects of SeIV and SeNPs. In *P. roqueforti*, SEM images reveal that SeNPs cause severe hyphal fragmentation and surface erosion. Nanoparticle aggregates stick to cell walls, while SeIV leads to partial shrinkage while maintaining hyphal integrity. This matches the TBARS data, with 0.836 Abs for SeIV compared to 0.582 for SeNPs. This suggests that the combined physical and oxidative stress from SeNPs is greater than the biochemical impact of SeIV. For *P. citrinum*, both treatments cause similar damage. SeIV leads to large-scale pitting and leakage, while SeNPs create localized nanopores. TBARS values are close, with 0.496 for SeIV and 0.488 for SeNPs, confirming their nearly equal strength in causing damage. *Asp. niger* shows extreme hyphal breakdown under SeNPs, leaving behind skeletal remnants. This is supported by a high TBARS value of 1.055 Abs. SeIV leads to moderate fracturing at 0.512 Abs, suggesting that SeNPs cause more lipid peroxidation. In *R. arrhizus*, SeIV results in uneven surface corrosion, while SeNPs uniformly thin the hyphal walls. TBARS data shows 0.465 for SeIV and 0.498 for SeNPs, indicating that SeNPs have a slight advantage through their sustained oxidative and abrasive effects. *Trichoderma spp.* shows partial hyphal damage from both treatments, with SeNPs adhering more and SeIV causing larger fractures. Similar TBARS values, 0.467 for SeIV and 0.483 for SeNPs, indicate this strain's resilience, likely due to its biocontrol adaptations.

At the molecular level, SeNPs generate ROS, which disrupt fungal membranes, proteins, and DNA. They also bind ergosterol. Smaller particles, sized 45 to 100 nm, improve uptake (Wadhwani *et al.*, 2016). SeIV quickly inactivates thiol groups in enzymes and causes DNA breaks, showing stronger effects at lower doses (Zhang *et al.*, 2020). These mechanisms lead to strong antifungal activity, as shown in TBARS and SEM data.

These findings show that SeNPs generally cause greater physical damage, while SeIV leads to quicker biochemical harm. The relationship between the structural changes seen with SEM and the oxidative stress measured by TBARS highlights the specific weaknesses of each strain. *Asp. niger* is the most vulnerable to SeNPs, while *P. roqueforti* is more affected by SeIV. These insights suggest that different forms of selenium can be tailored for antifungal strategies, warranting more studies on the underlying mechanisms.

In contrast, SeNPs and Se(IV) exert antifungal activity through distinct molecular interactions with fungal cells. SeNPs generate reactive oxygen species (ROS), disrupting membranes, proteins, and DNA, while binding ergosterol to increase permeability and inhibiting cytochrome P450, impairing detoxification (Husen & Siddiqi, 2014; Kieliszek, 2019). Smaller SeNPs (45–100 nm) enhance ROS production and cellular uptake, amplifying damage, as seen in *Asp. niger* (TBARS: 1.055 Abs at 200 ppm) (Wadhwani *et al.*, 2016). SeIV, with higher solubility, rapidly inactivates thiol groups in enzymes like thioredoxin reductase, disrupting redox balance, and induces DNA breaks, showing stronger effects at lower doses (e.g., 50 ppm, TBARS: 0.486 Abs for *P. roqueforti*) (Zhang *et al.*, 2020; Hosnedlova *et al.*, 2018). These mechanisms, confirmed by SEM and TBARS, highlight SeIV's biochemical potency and SeNPs' combined physical-oxidative action.

7.2. The superior antifungal potency of selenite Se(IV) compared to selenium nanoparticles (SeNPs)

Selenite Se(IV) shows stronger antifungal activity at lower concentrations than selenium nanoparticles (SeNPs). This difference arises from their distinct chemical reactivity and action mechanisms. Se(IV) is more effective at lower doses, between 50 and 100 ppm, due to its high solubility and quick uptake by cells. This rapid action allows it to efficiently inactivate thiol groups and disrupt redox processes, resulting in 70 to 90% fungal inhibition (Zhang *et al.*, 2020). The TBARS data support this, showing that Se(IV) causes greater oxidative stress at 50 ppm, with 0.486 abs for *P. roqueforti* compared to 0.121 abs for SeNPs. SeNPs diffuse and aggregate more slowly, especially larger particles ranging from 150 to 275 nm, which requires higher doses to achieve similar effectiveness (Wadhwani *et al.*, 2016). Se(IV)'s fast biochemical action contrasts with the sustained reactive oxygen species (ROS) production and physical disruption of SeNPs. This makes Se(IV) suitable for acute treatments, while SeNPs are better for long-term applications like probiotics at doses under 50 ppm

(Kieliszek *et al.*, 2015). However, Se(IV) has some downsides, such as higher toxicity to non-target organisms and possible environmental persistence. The characteristics that enhance Se(IV)'s effectiveness, like its solubility, reactivity, and bioavailability, also raise its ecological risks when compared to the more controlled action of SeNPs. This balance between effectiveness and safety needs careful evaluation when choosing selenium-based antifungal treatments.

In conclusion, the findings show that SeNPs and Se(IV) have strong antifungal effects against the five isolated fungal genera *Penicillium*, *Aspergillus*, *Rhizopus* and *Trichoderma*. It highlights the potential use of these selenium compounds as antifungal agents however, their varying efficacy depending on the used concentration and chemical form. Se(IV) works best at lower doses (50-100 ppm) for quick biochemical disruption, while SeNPs (45-100 nm) cause lasting physical and oxidative damage at 100-200 ppm. This makes them suitable for integrated fungal management. These strain-specific responses underscore that "one-size-fits-all" approaches fail in antifungal therapy. SeNPs excel against structurally vulnerable or antioxidant-deficient fungi (*P. roqueforti*, *A. niger*), while Se(IV) suits rapid strikes against adaptable strains (*P. citrinum*). Controlling fungal growth is crucial in agriculture, preventing crop spoilage and food preservation. In food preservation, SeNPs at less than 50 ppm can boost *Lactobacillus* growth for probiotic use and reduce foodborne pathogens, improving shelf life in coatings. Se(IV) is better for immediate treatments like post-harvest fumigation. These specific insights, backed by SEM and TBARS data, support customized, eco-friendly approaches in agriculture and food safety. The lower toxicity of SeNPs makes them favorable for sustainable use.

List of abbreviations:

SeNPs: Selenium nanoparticles

Se(IV): Selenite ions

ABT: *L. acidophilus*, *B. bifidum* and *S. thermophilus*

L. acidophilus: *Lactobacillus acidophilus*

B. bifidum: *Bifidobacterium bifidum*

S. thermophilus: *Streptococcus thermophilus*

A. niger: *Aspergillus niger*

P. roqueforti: *Penicillium roqueforti*

P. citrinum: *Penicillium citrinum*

R. arrhizus: *Rhizopus arrhizus*

Declarations

Ethics approval and consent to participate: All data, images, and materials included in the manuscript (e.g., fungal strains, ABT culture, experimental results) were obtained and used in accordance with applicable ethical guidelines and institutional permissions.

Consent for publication: The manuscript submitted for publication does not contain any material that is unlawful, defamatory, or which would, if published, in any way whatsoever, violate the terms and conditions as laid down in the publication agreement with The National Information and Documentation Centre (NIDOC) affiliated to Academy of Scientific Research and Technology (ASRT). The manuscript does not include any identifiable personal data, confidential information, or materials requiring third-party consent for publication.

Availability of data and material: available.

Competing interests: The authors declare that they have no conflict of interest in the publication.

Funding: Not applicable.

Authors' contributions:

Mohsen A. Zommara: Conceptualized the study, designed the experimental protocol, performed the synthesis and characterization of nano-selenium (SeNPs), and wrote the initial draft of the manuscript and critically reviewed and edited the manuscript for final submission.

Sherouq Sakar: Conducted the in vitro antifungal experiments, analyzed the data, and prepared the figures and tables for the manuscript.

Elsayed B. Blal: Provided expertise in mycology, performed statistical analysis of the antifungal effects, contributed to the interpretation of results and revised the manuscript for intellectual content..

Metwaly Salim: Provided expertise in mycology, validated the fungal species used.

Nabil Algamal: Cultured and maintained the ABT culture and fungal species.

All authors read and agree for submission of manuscript to the journal.

References

- Ayad, E. H. E., Nashat, S., El-Sadek, N., Metwaly, H. and El-Soda, M. (2004) Selection of wild lactic acid bacteria isolated from traditional Egyptian dairy products according to production and technological criteria. *Food Microbiol.*, 6: 715-725. doi:10.1016/j.fm.2004.02.009.

- Bafana, A., Kumar, G., and Kashyap, S. M. (2018). Biosynthesis of selenium nanoparticles using *Aspergillus niger* and their antifungal activity against pathogenic fungi. *J. Cluster Sci.*, 29(5), 867-873.
- Barkalina, N., Charalambous, C., Jones, C., & Coward, K. (2014). Nanotechnology in reproductive medicine: Emerging applications of nanomaterials. *Nanomedicine: Nanotechnology, Biology and Medicine*, 10(5), e921–e938. <https://doi.org/10.1016/j.nano.2014.01.001>
- Blinova, A., Blinov, A., Kravtsov, A., Nagdalian, A., Rekhman, Z., Gvozdenko, A., Kolodkin, M., Filippov, D., Askerova, A., Golik, A., et al. (2023). Synthesis, characterization and potential antimicrobial activity of selenium nanoparticles stabilized with vetyltrimethyl ammonium chloride. *Nanomaterials*, 13, 3128.
- Borman, A. M., et al. (2012). Clinical and laboratory features of mucormycosis caused by *Rhizopus arrhizus*. *J. Clin. Microbiol.*, 50(5), 1699-1704.
- Bose, P., and Pandey, A. (2016). Industrial applications of *Rhizopus arrhizus* in the production of organic acids and enzymes. *Biochem. Eng. J.*, 106, 1-13.
- Cairns, T. C., Nai, C. and Meyer, V. (2018). How a fungus shapes biotechnology: 100 years of *Aspergillus niger* research. *Fungal Biol Biotechnol* 5, 13. <https://doi.org/10.1186/s40694-018-0054-5>.
- Colavolpe, M. B., Mejía, S. J. and Albertó, E. (2015). Efficiency of treatments for controlling *Trichoderma* spp during spawning in cultivation of lignicolous mushrooms. *Braz. J. Microbiol.*, 45:1263-70. doi: 10.1590/s1517-83822014000400017.
- Dave, R. I., and Shah, N. P. (1996). Evaluation of media for selective enumeration of *Streptococcus thermophilus*, *Lactobacillus delbrueckii* subsp. *bulgaricus*, *Lactobacillus acidophilus*, and *Bifidobacterium* species. *J Dairy Sci.*, 79(9), 1529-1536. [https://doi.org/10.3168/jds.S0022-0302\(96\)76513-2](https://doi.org/10.3168/jds.S0022-0302(96)76513-2).
- Devi, M. S., Srinivasan, S., Muthuvel, A. (2023). Selenium nanomaterial is a promising nanotechnology for biomedical and environmental remediation: A detailed review, *Biocatal. Agric. Biotechnol.*, 51, 102766, <https://doi.org/10.1016/j.bcab.2023.102766>.
- Dworecka-Kaszak, B., Biegańska, M. J., Dąbrowska, I. (2020). Occurrence of various pathogenic and opportunistic fungi in skin diseases of domestic animals: a retrospective study. *BMC Vet Res.*, 16:248. doi: 10.1186/s12917-020-02460-x.
- El-Saadony, M. T., Saad, A. M., Taha, T. F., Najjar, A.A., Zabermawi, N.M., Nader, M.M.; AbuQamar, S.F., El-Tarabily, K.A. and Salama, A. (2021). Selenium nanoparticles from *Lactobacillus paracasei* HM1 capable of antagonizing animal pathogenic fungi as a new source from human breast milk. *Saudi J. Biol. Sci.*, 28: 6782–6794. doi:10.1016/j.sjbs.2021.07.059
- Fisher, M. C., Henk, D. A., Briggs, C. J., Brownstein, J. S., Madoff, L. C., McCraw, S. L and Gurr, S. J. (2012). Emerging fungal threats to animal, plant and ecosystem health. *Nature*. 484:186-94. doi: 10.1038/nature10947.
- Fleming, A. (1929). On the Antibacterial Action of Cultures of a *Penicillium*, with Special Reference to Their Use in the Isolation of *B. influenzae*. *Br. J. Exp. Pathol.*, 10(3), 226-236.
- Fourest, E., Canal, C. and Roux, J. C. (1994). Improvement of heavy metal biosorption by mycelial dead biomasses (*Rhizopus arrhizus*, *Mucor miehei* and *Penicillium chrysogenum*): pH control and cationic activation. *FEMS Microbiol Rev.*, 14(4):325-32. doi: 10.1111/j.1574-6976.1994.tb00106.x.
- Gharieb, M. M., Soliman, A. M. and Omara, M. S. (2025). Biosynthesis of selenium nanoparticles by potential endophytic fungi *Penicillium citrinum* and *Rhizopus arrhizus*: characterization and maximization. *Biomass Conv. Bioref.* 15, 2319–2328. <https://doi.org/10.1007/s13399-023-05084-x>
- Ghosh, B., and Ray, R. R. (2011). Current commercial perspective of *Rhizopus oryzae*: A review. *J. Appl. Sci.*, 11(14), 2470-2486. <https://doi.org/10.3923/jas.2011.2470.2486>.
- Gobbetti, M., De Angelis, M., Di Cagno, R., Mancini, L., and Fox, P. F. (2015). The Microbiology of Traditional Fermented Dairy Products. *J. Dairy Sci.*, 98(5), 2985-3002.
- Hamouda, R.A., Abdel-Hamid, M.S., Hagagy, N., & Nofal, A.M. (2024). The Potent Effect of Selenium Nanoparticles: Insight into the Antifungal Activity and Preservation of Postharvest Strawberries from Gray Mold. *Journal of the Science of Food and Agriculture*, 104(11), 6756–6768. <https://doi.org/10.1002/jsfa.13502>

- Hosnedlova, B., Kepinska, M., Skalickova, S., Fernandez, C., Ruttkay-Nedecky, B., Peng, Q., Baron, M., Melcova, M., Opatrilova, R., Zidkova, J., Björklund, G., Sochor, J. and Kizek, R. (2018). Nano-selenium and its nanomedicine applications: a critical review. *Int J Nanomedicine*, 13:2107-2128. doi: 10.2147/IJN.S157541.
- Husen, A., & Siddiqi, K. S. (2014). Phytosynthesis of nanoparticles: Concept, controversy and application. *Nanoscale Research Letters*, 9(1), 229. <https://doi.org/10.1186/1556-276X-9-229>
- Hymery, N., Vasseur, V., Coton, M., Mounier, J., Jany, J. L., Barbier, G. and Coton, E. (2014). Filamentous Fungi and Mycotoxins in Cheese: A Review. *Compr Rev Food Sci Food Saf.*, 13:437-456. doi: 10.1111/1541-4337.12069. PMID: 33412699.
- Islam, S. N., Naqvi, S. M. A., Raza, A., Jaiswal, A., Singh, A. K., Dixit, M., Barnwal, A., Gambhir, S. and Ahmad, A. (2022). Mycosynthesis of highly fluorescent selenium nanoparticles from *Fusarium oxysporum*, their antifungal activity against black fungus *Aspergillus niger*, and in-vivo biodistribution studies. *3 Biotech.*; 12(11):309. doi: 10.1007/s13205-022-03383-0.
- Jangid, H., Garg, S., Kashyap, P., Karnwal, A., Shidiki, A. and Kumar G. (2024). Bioprospecting of *Aspergillus* sp. as a promising repository for anti-cancer agents: a comprehensive bibliometric investigation. *Front Microbiol.*;15:1379602. doi: 10.3389/fmicb.2024.1379602.
- Kamle, M., Mahato, D. K., Gupta, A., Pandhi, S., Sharma, N., Sharma, B., Mishra, S., Arora, S., Selvakumar, R., Saurabh, V., Dhakane-Lad, J., Kumar, M., Barua, S., Kumar, A., Gamlath, S. and Kumar P. (2022). Citrinin mycotoxin contamination in food and feed: impact on agriculture, human health, and detection and management strategies. *Toxins (Basel)*.; 14(2):85. doi: 10.3390/toxins14020085.
- Karthik, K. K., Cheriyan, B. V., Rajeshkumar, S. and Gopalakrishnan, M. (2024). A review on selenium nanoparticles and their biomedical applications, *Biomed. Technol.*, 6: 61-74. doi.:10.1016/j.bmt.2023.12.001.
- Kazempour, Z., Hashemian, A., and Pourjam, E. (2020). Antifungal Activity of Selenium Nanoparticles Synthesized by *Bacillus subtilis* Against *Aspergillus niger*. *J. Plant Prot. Res.*, 60(3), 289-295.
- Khatoon, A., Khan, M., & Alzohairy, M. A. (2022). Biogenic SeNPs suppress sporangiospore formation in *Rhizopus arrhizus* through ROS-mediated DNA damage. *Scientific Reports*, 12, 15389. <https://doi.org/10.1038/s41598-022-19770-9>.
- Kieliszek, M. (2019). Selenium—fascinating microelement, properties and sources in food. *Molecules*, 24(7), 1298. <https://doi.org/10.3390/molecules24071298>
- Kieliszek, M., Błażej, S., Gientka, I., & Bzducha-Wróbel, A. (2015). Accumulation and metabolism of selenium by yeast cells. *Applied Microbiology and Biotechnology*, 99(13), 5373–5382. <https://doi.org/10.1007/s00253-015-6650-x>
- Kopel, J., Fralick, J. and Reid, T. W. (2022). The potential antiviral effects of selenium nanoparticles and coated surfaces. *Antibiotics*, 11:1683. doi: 10.3390/antibiotics11121683.
- Krausova G, Kana A, Vecka M, Hyrslova I, Stankova B, Kantorova V, Mrvikova I, Huttl M, Malinska H. (2021). *In Vivo* Bioavailability of Selenium in Selenium-Enriched *Streptococcus thermophilus* and *Enterococcus faecium* in CD IGS Rats. *Antioxidants (Basel)*.; 10(3):463. doi: 10.3390/antiox10030463.
- Kure, C. F., and Skaar, I. (2019). The fungal problem in cheese industry. *Curr. Opin. Food Sci.* Elsevier Ltd. <https://doi.org/10.1016/j.cofs.2019.07.003>
- Lei X, Peng Y, Li Y, Chen Q, Shen Z, Yin W, Lemiasheuski V, Xu S, He J. (2024). Effects of selenium nanoparticles produced by *Lactobacillus acidophilus* HN23 on lipid deposition in WRL68 cells. *Bioorg Chem.*; 145:107165. doi: 10.1016/j.bioorg.2024.107165.
- Martínez-Esquivias, F., Guzmán-Flores, J. M., Pérez-Larios, A., González Silva, N. and Becerra-Ruiz, J.S. (2021). A Review of the antimicrobial activity of selenium nanoparticles. *J. Nanosci. Nanotechnol.*, 21: 5383–5398. doi: 10.1166/jnn.2021.19471.
- Moglad, E. H., Al-Hakimi, A. N., and Al-Sheikh, Y. A. (2023). Isolation and biological activities of chemical constituents from *Aspergillus niger* Ma001. *J. Fungi*, 9(3), 326. <https://doi.org/10.3390/jof9030326>.
- Moreno-Martin G, Pescuma M, Pérez-Corona T, Mozzi F, Madrid Y. (2017). Determination of size and mass-and number-based concentration of biogenic SeNPs synthesized by lactic acid bacteria by using a multimethod approach. *Anal Chim Acta.*; 992:34-41. doi: 10.1016/j.aca.2017.09.033.

- Mousavi, B., Hedayati, M. T., Hedayati, N., Ilkit, M. and Syedmousavi S. (2016). Aspergillus species in indoor environments and their possible occupational and public health hazards. *Curr Med Mycol.* 2(1):36-42. doi: 10.18869/acadpub.cmm.2.1.36.
- Nagy, G., Pinczes, G., Pinter, G., Pócsi, I., Prokisch, J. and Banfalvi G. (2016). In situ electron microscopy of lactomicroselenium particles in probiotic bacteria. *Int. J. Mol. Sci.*, 17:1047-1055. doi:10.3390/ijms17071047.
- Nandini, B., Hariprasad, P., Prakash, H. S., Shetty, H. S. and Geetha, N. (2017). Trichogenic-selenium nanoparticles enhance disease suppressive ability of Trichoderma against downy mildew disease caused by *Sclerospora graminicola* in pearl millet. *Sci Rep.*;7(1):2612. doi: 10.1038/s41598-017-02737-6.
- Nile, S. H., Thombre, D., Shelar, A., Gosavi, K., Sangshetti, J., Zhang, W., Sieniawska, E., Patil, R. and Kai, G. (2023). Antifungal properties of biogenic selenium nanoparticles functionalized with nystatin for the inhibition of *Candida albicans* Biofilm Formation. *Molecules.*, 28:1836. doi: 10.3390/molecules28041836.
- Normand, A. C., Cassagne, C., Gautier, M., Becker, P., Ranque, S., Hendrickx, M., & Piarroux, R. (2017). Decision criteria for MALDI-TOF MS-based identification of filamentous fungi using commercial and in-house reference databases. *BMC Microbiology*, 17(1), 25. <https://doi.org/10.1186/s12866-017-0937-2>
- Patterson, T. F., Thompson, G. R. 3rd, Denning, D. W., Fishman, J. A., Hadley, S., Herbrecht, R., Kontoyiannis, D. P., Marr, K. A., Morrison, V. A., Nguyen, M. H., Segal, B. H., et al. (2016). Practice guidelines for the diagnosis and management of aspergillosis: 2016 update by the infectious diseases society of america. *Clin Infect Dis.*; 63(4):e1-e60. doi: 10.1093/cid/ciw326.
- Perrone, G. and Susca, A. (2017). Penicillium species and their associated mycotoxins. *Methods Mol Biol.*, 1542:107-119. doi: 10.1007/978-1-4939-6707-0-5.
- Pitt, J. I., and Hocking, A. D. (2009). Fungi and food spoilage (3rd ed.). Springer. <https://doi.org/10.1007/978-0-387-92207-2>.
- Prokisch, J. and Zommara, M. (2011). Process for producing elemental selenium nanospheres. United States Patent 8,003,071.
- Ráduly, Z., Szabó, L., Madar, A., Pócsi, I. and Csernoch, L. (2020). Toxicological and medical aspects of aspergillus-derived mycotoxins entering the feed and food chain. *Front Microbiol.*;10:2908. doi: 10.3389/fmicb.2019.02908.
- Sabino, R., Veríssimo, C., Viegas, C., Viegas, S., Brandão, J., Alves-Correia, M., Borrego, L. M., Clemons, K. V., Stevens, D. A and Richardson, M. (2019). The role of occupational Aspergillus exposure in the development of diseases. *Med Mycol.*;57(Supplement_2):S196-S205. doi: 10.1093/mmy/myy090.
- Salama HH, El-Sayed HS, Abd-RabouNS, Hassan ZMR. (2021). Production and use of eco-friendly selenium nanoparticles in the fortification of yoghurt. *J. Food Process Preserv.*; 45:e15510. <https://doi.org/10.1111/jfpp.15510>.
- Samer Y. Alqaraleh, Wael A. Al-Zereini, Nesrin R. Mwafi, Sahar M. Jaffal, Aiman I. Al-Qtaitat. (2024). The green synthesis of selenium nanoparticles: A comprehensive review on methodology, Characterization and biomedical applications. *Res. J. Pharm. Tech.*; 17(8):4054-2. doi: 10.52711/0974-360X.2024.00629
- Sampath S, Sunderam V, Manjusha M, Dlamini Z, Lawrance AV. (2024). Selenium Nanoparticles: A Comprehensive Examination of Synthesis Techniques and Their Diverse Applications in Medical Research and Toxicology Studies. *Molecules.*, 29(4):801. doi: 10.3390/molecules29040801.
- Santos, C., Paterson, R. R. M., Venâncio, A., & Lima, N. (2010). Filamentous fungal characterizations by matrix-assisted laser desorption/ionization time-of-flight mass spectrometry. *Journal of Applied Microbiology*, 108(2), 375–385. <https://doi.org/10.1111/j.1365-2672.2009.04448.x>
- Schuster, E., Dunn-Coleman, N., Frisvad, J. C., & van Dijck, P. W. M. (2024). On the safety of *Aspergillus niger* - a review. *Appl. Microbiol. Biotechnol.*, 108, 1-14. <https://doi.org/10.1007/s00253-024-13245-2>.
- Serov, D. A., Khabatova, V. V., Vodeneev, V., Li, R., & Gudkov, S. V. (2023). A review of the antibacterial, fungicidal and antiviral properties of selenium nanoparticles. *Materials*, 16(15), 5363. <https://doi.org/10.3390/ma16155363>.
- Syedmousavi S, Bosco SMG, de Hoog S, Ebel F, Elad D, Gomes RR, Jacobsen ID, Jensen HE, Martel A, Mignon B, Pasmans F, Piecková E, Rodrigues AM, Singh K, Vicente VA, Wibbelt G, Wiederhold NP, Guillot J. (2018). Fungal infections in animals: a patchwork of different situations. *Med Mycol.*, 56:165-187. doi: 10.1093/mmy/myx104.

- Shakibaie, M., Forootanfar, H., Golkari, Y., Mohammadi-Khorsand, T., & Shakibaie, M. R. (2015). Anti-biofilm activity of biogenic selenium nanoparticles and selenium dioxide against clinical isolates of *Staphylococcus aureus*, *Pseudomonas aeruginosa*, and *Proteus mirabilis*. *Journal of Trace Elements in Medicine and Biology*, 29, 235–241. <https://doi.org/10.1016/j.jtemb.2014.07.014>
- Silva, L. J. G., Pereira, A. M. P. T., Pena, A., & Lino, C. M. (2021). Citrinin in Foods and Supplements: A Review of Occurrence and Analytical Methodologies. *Foods*, 10(1), 14. <https://doi.org/10.3390/foods10010014>.
- Singhal N, Kumar M, Kanaujia PK, Virdi JS. (2015). MALDI-TOF mass spectrometry: an emerging technology for microbial identification and diagnosis. *Front Microbiol.*, 6:791. doi: 10.3389/fmicb.2015.00791.
- SPSS. SPSS for windows. statistical package for social studies 567 Software; Version 24; Ibm Corp. Armonk, Ny, USA; (2016).
- Vahdati, M., & Moghadam, T. T. (2020). Synthesis and characterization of selenium nanoparticles and their effects on biofilm formation. *Journal of Nanostructures*, 10(1), 34–42. <https://doi.org/10.22052/JNS.2020.01.004>
- Vahdati, M., & Tohidi Moghadam, T. (2023). A Review of the Antibacterial, Fungicidal and Antiviral Properties of Selenium Nanoparticles. *Nanomaterials*, 13(15), 2196. <https://doi.org/10.3390/nano13152196>
- Vázquez, M. B., Cepeda, A., Franco, C. M., & Fente, C. A. (2021). Fungal contamination in cheese: Molecular identification and antifungal susceptibility. *J. Dairy Res.*, 88(2), 165-170. <https://doi.org/10.1017/S0022029921000324>.
- Voloshchuk, N., Irakoze, Z., Kang, S., Kellogg, J. J., & Wee, J. (2024). Three ecological models to evaluate the effectiveness of trichoderma spp. for suppressing aflatoxigenic *Aspergillus flavus* and *Aspergillus parasiticus*. *Toxins*, 16(7), 314. <https://doi.org/10.3390/toxins16070314>.
- Wadhvani, S. A., Shedbalkar, U. U., Singh, R., & Chopade, B. A. (2016). Biogenic selenium nanoparticles: Current status and future prospects. *Applied Microbiology and Biotechnology*, 100(6), 2555–2566. <https://doi.org/10.1007/s00253-016-7300-7>
- Wang L, Hu C, Shao L. (2017). The antimicrobial activity of nanoparticles: present situation and prospects for the future. *Int J Nanomedicine*, 12:1227-1249. doi: 10.2147/IJN.S121956.
- Wang, L., Zhang, H., & Zhang, X. (2016). Effects of Selenium on the Growth and Mycotoxin Production of *Penicillium expansum*. *Food Chem.*, 197(Part A), 1125-1131.
- Wheat PF. (2001). History and development of antimicrobial susceptibility testing methodology. *J Antimicrob Chemother.*; 48 Suppl 1:1-4. doi: 10.1093/jac/48.suppl_1.1.
- Woo S. L., Hermosa R., Lorito, M. et al. (2023). Trichoderma: a multipurpose, plant-beneficial microorganism for eco-sustainable agriculture. *Nat. Rev. Microbiol.*, 21: 312-326. <https://doi.org/10.1038/s41579-022-00819-5>
- Xu, C. (2020). Green Synthesis of Selenium Nanoparticles (SeNPs) Via Environment-Friendly Biological Entities. In: Saquib, Q., Faisal, M., Al-Khedhairi, A.A., Alatar, A.A. (eds) *Green Synthesis of Nanoparticles: Applications and Prospects*. Springer, Singapore. https://doi.org/10.1007/978-981-15-5179-6_11
- Yapar N. (2014). Epidemiology and risk factors for invasive candidiasis. *Ther. Clin. Risk Manag.*;10:95-105. doi: 10.2147/TCRM.S40160.
- Zhang, H., Li, Z., Dai, C., Wang, P., Fan, S., Yu, B., & Qu, Y. (2021). Selenium-enriched *Bacillus subtilis* reduces the incidence of colorectal cancer in a mouse model by inhibiting the β -catenin/FOS signaling pathway. *Frontiers in Oncology*, 11, 765817. <https://doi.org/10.3389/fonc.2021.765817>
- Zhang, J., Wang, X., & Xu, T. (2020). Selenium in fungal physiology and pathogenicity: A review. *Fungal Biology Reviews*, 34(2), 71–81. <https://doi.org/10.1016/j.fbr.2020.01.002>
- Zhang, J., Wang, X., & Xu, T. (2020). SEM protocols for fungal antifungal studies. *Nanomaterials*, 10(5), 948. <https://doi.org/10.3390/nano10050948>.
- Zhang, S., Liao, S., Yu, X., Lu, H., & Zhang, F. (2020). Enhanced fumaric acid production by *Rhizopus arrhizus* through acidic pH stress adaptation. *Appl. Biochem. Biotechnol.*, 192(2), 658-670. <https://doi.org/10.1007/s12010-020-03346-7>
- Zhao, X., and Chen, S. (2019). Fermentative production of lactic acid from lignocellulosic biomass by *Rhizopus arrhizus*: Process optimization and biotechnological applications. *Biotechnol. Adv.*, 37(2), 137-145.

- Zhu T., Meng T., Zhan, J., Zhong W., Müller C. and Cai Z., (2015). Fungi-dominant heterotrophic nitrification in a subtropical forest soil of China. *J. Soils and Sediments.*, 15:705-709. doi:10.1007/s11368-014-1048-4.
- Zommara M, Tachibana N, Mitsui K, Nakatani N, Sakono M, Ikeda I, Imaizumi K. Inhibitory effect of ethanolamine plasmalogen on iron- and copper-dependent lipid peroxidation. *Free Radic Biol Med.* 1995 Mar;18(3):599-602. doi: 10.1016/0891-5849(94)00155-d.
- Zommara, M. A., Prokisch, J., El-Ghaish, S. N., & Abdelaziz, A. M. (2018). Biological production of selenium nanoparticles by yoghurt culture: A novel source of selenium dietary supplement. *Egyptian J. Dairy Sci.*, 46(Suppl), S31–S39.
- Zommara, M., Omran, M. and Ghanimah, M. (2022). Milk permeate medium for the production of selenium nanoparticles by lactic acid bacteria. *Int. J. Dairy Tech.*, 75, 603-610. doi: 10.1111/1471-0307.12875
- Zommara, M.; Abd El-Aziz, A. M.; Elgammal, N. A.; Prokisch, J. and Swelam, S. (2021). In vitro biosynthesis of organic selenium by *Lactobacillus casei* from inorganic selenium forms. *Rom. Biotechnol. Lett.*, 26(5): 2916-2925. doi: 10.25083/rbl/26.5/2916-2925.